HYDROTHERMAL ALTERATION, MASS TRANSFER AND MAGNETITE MINERALIZATION IN DEXTRAL SHEAR ZONES, WESTERN HUDSON HIGHLANDS, NY

By Michael J. Kalczynski

A thesis submitted to the

Graduate School-Newark

Rutgers, The State University of New Jersey

in partial fulfillment of requirements

for the degree of

Master of Science

Graduate Program in Geology

Written under the direction of

Professor Alexander E. Gates

and approved by

_____

_____

_____

Newark, New Jersey

May 2012

Hydrothermal Alteration, Mass Transfer and Magnetite Mineralization in Dextral Shear Zones, Western Hudson Highlands, NY

By Michael J. Kalczynski

Thesis Director: Professor Alexander E. Gates

Massive magnetite 'veins' formed during hydrothermal mineralization within northeast trending dextral shear zones in the crystalline bedrock of the western Hudson Highlands, New York. The veins formed in right step-over dilational jogs during the late stages of movement, in an open fracture system. Acidic metamorphic fluids derived from metavolcanic country rock and saturated with iron, flushed through fractures, reacted with wall rock, and exchanged chemical species. Buffered by the composition of the local country rock, fluids migrated and mixed along the fault during seismically induced 'pumping' events. The fluids migrated and deposited varying gangue mineral assemblages in favorable conditions in the dilated fractures. These assemblages reflect the changing flux, fluid buffering source, and/or physical conditions.

Three distinct zones formed through this process. The wall rock adjacent to the vein was altered to form a 'bleached' zone. The vein contains an outer 'layered' zone of ferromagnesian-rich bands, and a core of 'massive' magnetite ore and gangue minerals. Bleached zones are dominated by amphibole and/or pyroxene, including scapolite, biotite, and apatite, within metavolcanic and quartzofeldspathic gneiss, or phlogopite and calcite within calc-silicate country rock. Calc-silicate layered and massive assemblages contain clinopyroxene, calcite, amphibole, and/or biotite or phlogopite.

Quartzofeldspathic and metavolcanic layered and massive assemblages are dominated by amphibole and/or orthopyroxene, with quartz and/or sulfides and calcite locally. Both assemblages contain magnetite, including the massive ore, central to the deposits.

Geochemical modeling of the bleached zone shows overall gains in volume (2.5-20.3%) and mass (3.1-18.1g relative to 100g of wall rock). In all instances, iron (2.4-5.3g), magnesium (1.0-2.8g), and calcium (0.6-6.5g), were gained, more so in calc-silicate adjacent deposits. Deposits adjacent to quartzofeldspathic country rock had large gains in silica (4.4-7.4g), whereas deposits in/near mafic metavolcanic rock lost silica (1.4-3.8g). Based on the mobility of silica, fluid fluxes were calculated between 5.3×10^5 to 6.6×10^6 cm^3/cm^2 for bleached zone alteration, large enough for significant element transport. Elements in abundance in the country rock contributed to the composition of the deposits, dominantly silica, calcium and sulfides.

AKNOWLEDGEMENTS

Thanks to Alec Gates for his reviews, support, advice, and patience throughout my graduate career. Thanks to Matt Gorring and Marian Lupulescu for all their support and for serving on this thesis committee. Special thanks extended to my undergraduate advisors, official and not, Gary Solar, Dave Valentino, and Jeff Chiarenzelli for teaching me the real meaning of research, in the lab and the field. I would also like to thank Mark Feigenson for technical support, and all the faculty, staff, and students of the Earth and Environmental Science Department at Rutgers-Newark for moral support. A special thanks to Roxanne for all the support.

TABLE OF CONTENTS

LIST OF TABLES

LIST OF FIGURES

INTRODUCTION

The Hudson Highlands in southeastern New York, host hundreds of iron deposits (Foose and McLelland, 1995; Puffer, 2001) that were extensively mined throughout the eighteenth and nineteenth centuries. The Highlands are located within the Reading Prong, a Grenville basement massif that forms part of the spine of the Appalachians within New York and New Jersey, extending into Pennsylvania and Connecticut. The Highlands also connect the Grenville basement massif Blue Ridge Mountains in the south and Green Mountains in the north (Fig. 1) (Gates *et al.,* 2006).

The Highlands contain many types of magnetite deposits (e.g. Hotz, 1954; Sims, 1958; Buddington, 1966; Gundersen, 2000, 2004; Puffer, 2001), reflecting multiple modes of emplacement (Hagner and Collins, 1955; Hagner *et al.*, 1963; Collins, 1969; Baker and Buddington, 1970; Foose and McLelland, 1995; Puffer and Gorring, 2005). Gundersen (2000) and Puffer (2001) acknowledge vein deposits created by hydrothermal remobilization of magnetite into faults and fractures, as well as deposits that are related to plutonic rocks. In this study, two ~3 to 5 km long 'veins', formed by hydrothermal mineralization, containing massive magnetite bodies within shear zones were analyzed. The northeast trending dextral shear zones and veins, formed late in the Grenville orogenic cycle (Gates, 1995), and are exposed at several abandoned magnetite mines within Harriman State Park, New York.

The extent of mineralization, element transport, and the deformationally enhanced fluid-rock interactions in the fault rocks and their host lithologies were analyzed to model their formation. Geochemical and petrological evidence leads to an interpretation of the formation and chemical evolution of the fluids and vein deposits. Mass transfer modeling is applied to wall rock geochemistry, to constrain the chemistry of the fluids responsible

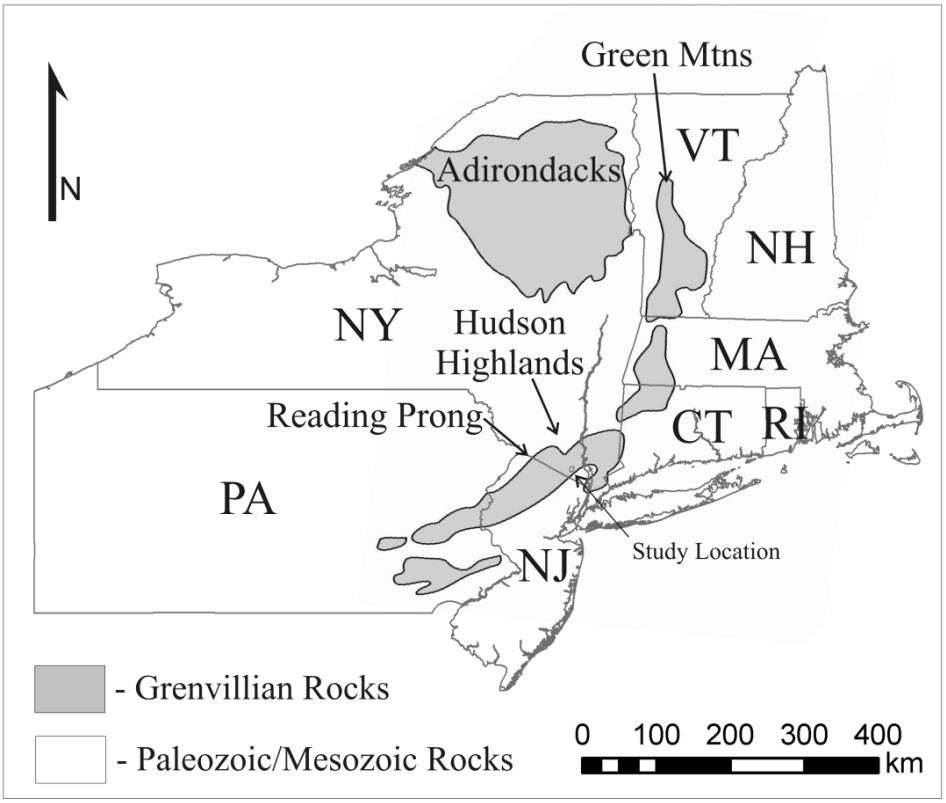

Figure 1. Map of the Northeastern United States showing distribution of Appalachian/Grenville rocks, The Reading Prong, Hudson Highlands, and study location.

for the deposits within the shear zones. Finally, a model for the development of the vein deposits is proposed.

GEOLOGY OF THE HUDSON HIGHLANDS

Several models currently exist for the formation of the crystalline bedrock of the Hudson Highlands. Bayley (1910) proposed that these rocks were derived from both plutons and metamorphosed sediments. More recent geochemical investigations found that some of the rocks are of plutonic origin (Gundersen, 2004; Volkert and Drake, 1999; Volkert, 2001; Gates *et al.*, 2006), but, based upon major element geochemistry, some of the layered gneisses have been interpreted to be volcanic (Helenek, 1971; Drake, 1984; Puffer and Gorring, 2005; Gates *et al.*, 2006). Gundersen (2004), and Volkert *et al.* (2010) proposed that many of these gneisses formed in an extensional backarc marginal

basin whereas others have a bimodal, volcanic origin. Gates *et al.* (2006) proposed formation of a volcanic pile with a volcaniclastic apron in an island arc or marine magmatic arc setting.

According to Gates *et al.* (2006), a volcanic pile formed in an arc setting around 1.29 to 1.25 Ga (Volkert *et al.*, 2010), characterized by layered intermediate and mafic rocks, associated plutons, and volcaniclastic sediments. Continental collision of the arc with another continent occurred during the building of the Rodinian supercontinent, ~1,050 to 1,020 Ma (Gates *et al.* 2006). This sequence underwent granulite facies metamorphism, between 1,045 to 1,024 Ma associated with the Ottawan phase of the Grenville orogeny (Volkert *et al.*, 2010). Locally, anatexis produced migmatites, granite sheets, and the early pegmatites (Gates *et al.*, 2006). Subsequent diorite intrusions occurred around 1,008 Ma, either the result of delamination at the end stages of the collision event, or the early dilational stages of the second tectonic event (Gates *et al.*, 2006). This second event is characterized by dextral strike-slip movement during a period of rapid uplift and unroofing at approximately 1,008 Ma to 924 Ma (Gates and Krol, 1998). Thick anastomosing zones of near vertical mylonite overprinted early shallowly dipping foliations. Dextral offset was on the order of several hundred kilometers (Gates *et al.*, 2006).

Geologic mapping in this region sub-divides the abundant quartzofeldspathic gneisses based upon the individual varietal ferromagnesian minerals (Dodd, 1965; Dallmeyer, 1974). However, considering that 80% of these rocks are quartz-feldspar gneisses (Gates *et al.,* 2006), this paper will follow the system proposed by Gundersen (1986), and adapted by Gates *et al.* (2006), using a type of sequence stratigraphy for metamorphic rocks. Units are grouped into lithofacies based on various rock types, to

define quartzofeldspathic, metasedimentary (calc-silicate, metapelite, and metapsammite) and metavolcanic (plagioclase-amphibole-pyroxene) assemblages (Fig. 2).

Metavolcanic Gneiss

The metavolcanic unit consists of strongly banded sequences of inter-layered mafic and intermediate gneisses, interpreted to represent rocks with volcanic protoliths (Gates *et al.,* 2006). Compositional banding ranges in thickness from 5 cm to 5 m with varying quantities of each rock type. Mafic assemblages are composed primarily of medium to coarse grained amphibole, plagioclase, clinopyroxene and enstatite, with minor sulfides and magnetite locally. Intermediate bands contain medium to coarse grained plagioclase and quartz, with minor amounts of amphibole, biotite, clinopyroxene and enstatite. This unit also contains localized interlayers of metasediments such as, quartzite, marble, and calc-silicate gneiss, as well as migmatites. The contacts with the quartzofeldspathic unit are interstratal gradational.

Quartzofeldspathic Gneiss

The quartzofeldspathic gneiss ranges from massive to layered quartz-plagioclase gneiss to quartz-K-feldspar-plagioclase gneiss with lesser amounts of clinopyroxene, enstatite, amphibole, and/or biotite. Minor amounts of magnetite and garnet also occur locally. Compositional layering is defined by the proportions and species of ferromagnesian minerals present. Closest to the contact with the metavolcanic unit, it is also locally interlayered with quartzite and amphibole-pyroxene mafic gneiss. Locally, this unit contains apparent fining upward sequences defined by an increase in the amount of biotite and decrease in the layer spacing, showing sharp contacts between sequences (Gates *et al.,* 2006). This could indicate that they are metasedimentary but it is difficult to interpret such relict sequences in granulite terranes. Gradational contacts with the

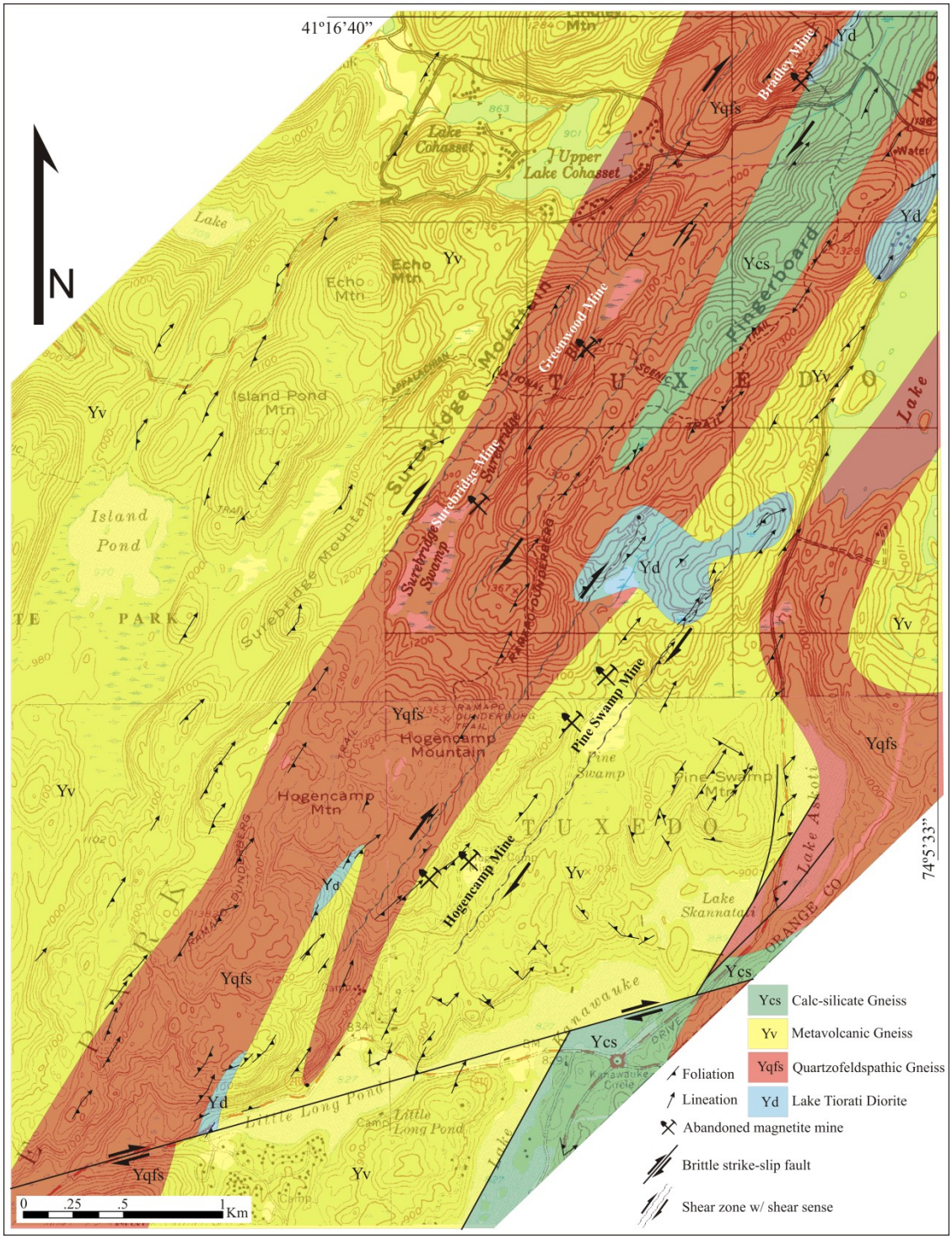

Figure 2. Geologic map of the study area, located within Harriman State Park, NY.

metavolcanic lithofacies, composition and mineralogy, and internal compositional layering suggest that this unit represents a volcaniclastic sequence (Gates *et al.,* 2006). Zircons analyzed from the quartzofeldspathic unit yield ages between 1,160 – 1,220 Ma for the zoned cores and between 1,000 - 1,080 Ma for the clear rims (Gates *et al.,* 2006).

Metasedimentary Gneiss

Throughout the western Hudson Highlands there are belts of rock considered to have sedimentary protoliths including metapelite, metapsammite, and calc-silicate gneisses interlayered with quartzite and marble. Belts of rock may contain varying amounts of these lithologies interlayered at the scale of meters to hundreds of meters (Gates *et al*., 2006). The calc-silicate gneiss is quartzofeldspathic containing diopside, K-feldspar, fluorapatite, titanite, scapolite, and amphibole. Ten's of centimeters up to meter-scale quartzite layers and discontinuous layers of diopside marble also occur in this unit. The metapelite consists of interlayered biotite-garnet gneiss with medium to coarse quartz, plagioclase, K-feldspar, and cordierite and sillimanite locally (Gates *et al.*, 2006). Zircons analyzed from the metasedimentary units yielded ages between 1,100 – 2,800 Ma for the zoned detrital cores and between 1,000 – 1,030 Ma for the distinct metamorphic rims (Gates *et al.,* 2006).

Lake Tiorati Diorite

Coarse to very-coarse grained disjunctively banded black and white diorite dikes and bodies containing plagioclase, orthopyroxene, clinopyroxene, interstitial amphibole, and minor biotite, occur throughout the field area. Hornblende rims clinopyroxene which armors orthopyroxene, however orthopyroxene does not occur within sheared bodies of the diorite, only disseminated clinopyroxene and hornblende. The diorite also grades to pyroxene-poor, anorthositic compositions locally (Gates *et al.,* 2003). Some small bodies

of diorite appear concentrated in certain areas, possibly indicating larger bodies at depth (Gates *et al.,* 2006).

Textures vary from coarse granoblastic to foliated and mylonitic with type II S-C fabrics (Lister and Snoke, 1984), exhibiting dextral shear sense (Fig. 3). Locally, the diorite contains xenoliths of gneiss, showing intimate, ductile contacts which are partially melted, forming a rind of coarse pegmatite granite around them. Granite also fills fractures in the diorite that opened after crystallization, but while the granite was still liquid (Gates *et al.,* 2006). Subhedral zircons with minimal to no zoning yielded a cluster of ages averaging 1,008 +/- 4 Ma (Gates *et al.,* 2006).

Figure 3. Lake Tiorati Diorite, with type II S-C fabrics and σ porphyroclasts indicating dextral shear sense.

Pegmatites

Two generations of pegmatites occur throughout the field area. The earliest dikes are white and contain K-feldspar, quartz, muscovite and minor garnet locally. They are concordant to semi-concordant to the gneissic foliation, commonly boudinaged and contain internal fabrics and deformed grains. Thickness of these dikes ranges from 1 cm

to 1 m. The later pegmatitic dikes are pink and very coarse grained, containing K-feldspar and quartz with muscovite, amphibole, magnetite, pyroxene, titanite, and/or garnet locally, depending on the rock intruded. They are highly discordant, commonly within brittle faults and contain xenoliths of gneiss, mylonites, and mineralized rock. They show minor to no deformational fabrics, and thickness ranges from 1 to 10 m. They are also associated with small granite bodies (Gates *et al.,* 2006). Ar/Ar thermochronology of hornblende from the later pegmatite yielded an age of 923 +/- 2.8 Ma, and an age of 794 +/- 3.0 Ma from biotite samples (Gates *et al.,* 2006).

MINERALIZED ZONES

Two shear zones, roughly half a kilometer wide, formed within a ~35-km-wide anastomosing dextral strike-slip shear system in the western Hudson Highlands (Gates *et al.,* 2004). Each one contains concordant to slightly discordant mineralized ore veins (Fig. 4). Both north-east trending zones are defined by steeply dipping foliations, penetrative mineral lineations, and type II S-C mylonites with dextral kinematic indicators (Fig. 3). The vein-wall rock contact is sharp and semi-concordant to the mylonitic foliation. However, on the small-scale it appears slightly discordant, crosses foliation, and has an uneven contact with wall rock.

The veins and their contacts are characterized by three distinct zones sub-parallel to the wall rock boundary (Fig. 5). The unaltered wall rock, grades into a 1 to 2 cm thick 'bleached zone' that is lighter in color and marked by the alteration of the original wall rock minerals. The bleached zone is also in direct contact with the mineralized vein. However, the bleached zone is not uniformly distributed throughout the deposits, and in some areas the mineralized vein is in direct contact with wall rock.

Figure 4. Map showing location of the shear zones and magnetite deposits.

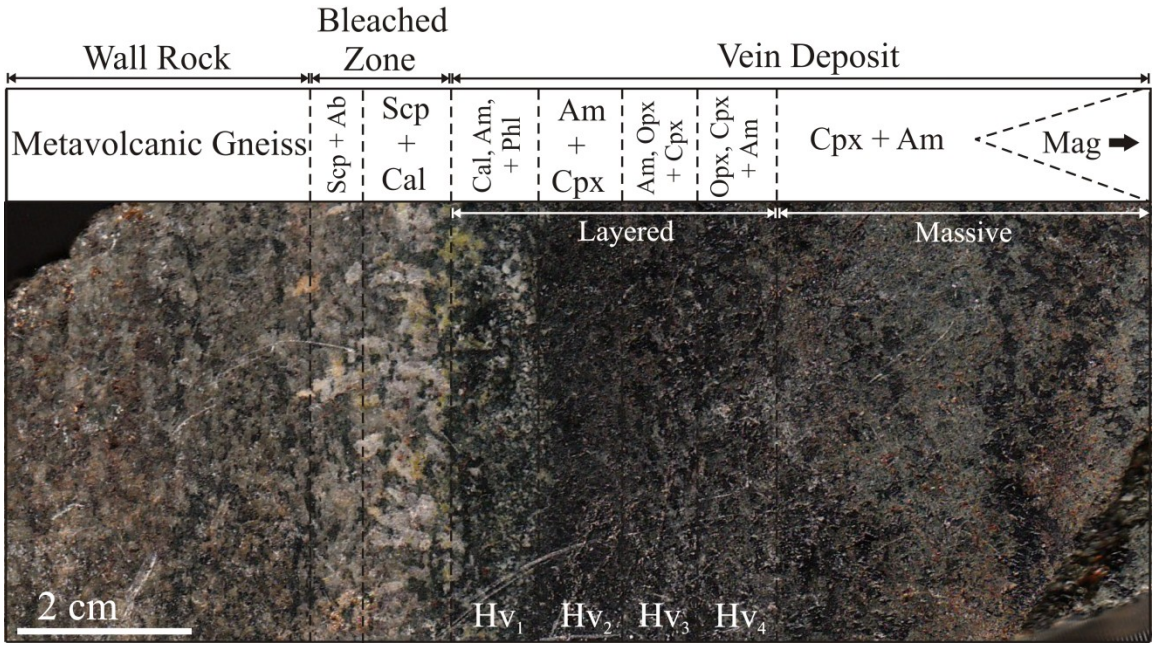

Figure 5. Hogencamp deposit sample, showing banded mineral assemblages across the wall rock, bleached zone, mineralized vein contact. Layered and massive vein, and layers Hv_1-Hv_4 are also shown.

The mineralized vein is characterized by two distinct zones, a layered sequence adjacent to the wall rock and a core of primarily very coarse, massive minerals (>2 cm in size). The layered sequence is characterized by distinct, dark colored bands of fine to medium grained, pyroxene, amphibole, and/or biotite-rich assemblages, which range in thickness from 2 to 10 cm and have gradational to sharp contacts. The individual bands are of assemblages dominated by pyroxene or amphibole.

The core of the veins consist of massive deposits, characterized by medium to very coarse, magnetite ore, randomly oriented amphibole and pyroxene gangue minerals, and late stage interstitial cementing minerals (Fig. 6). Thickness of the vein ranges from 2 to 15 m and from ~10 m, up to 1 km in length. The thickness of the ore zone ranges from 1 to 10 m and from ~100 to 500 m in length. The narrow zones that connect the magnetite deposits are typically composed of randomly oriented to aligned pyroxenes and amphiboles with minor magnetite, biotite, and/or quartz. The zones are commonly

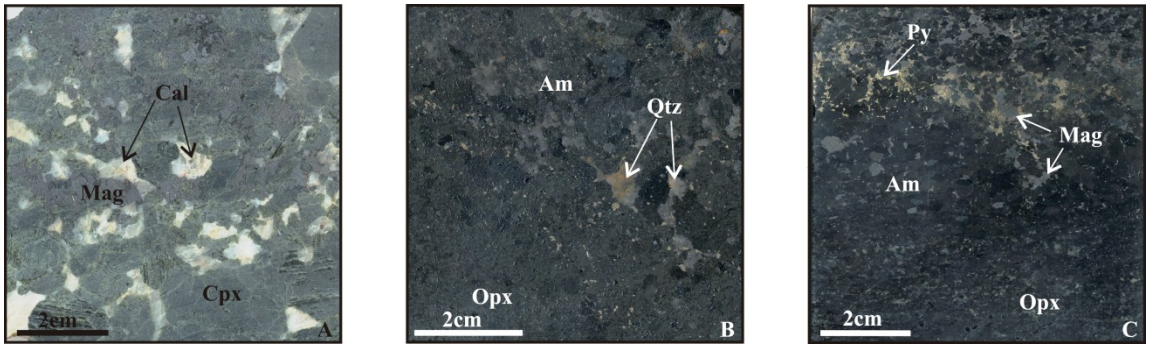

Figure 6. Massive vein assemblages from Hogencamp (A) and Greenwood Mines (B & C), showing late-stage interstitial cementing minerals; (A) calcite in massive clinopyroxene, (B) quartz in amphibole, orthopyroxene, and minor magnetite, and (C) pyrite in amphibole, magnetite, and layered orthopyroxene.

intruded by late pegmatite dikes that contain the mineralized rock as xenoliths.

Bleached zone mineral assemblages, vein material, and late-stage cementing minerals vary by location within each of the two mineralized shear zones. In areas of calcium-rich country rocks, clinopyroxene/calcite rich mineral assemblages dominate the bleached zone and the vein assemblages. In areas of quartzofeldspathic country rock, amphibole/quartz assemblages dominate the layered and massive vein material, whereas areas with iron and sulfide-rich country rocks (metavolcanics) contain orthopyroxene/sulfide-rich vein assemblages. Pyroxenes vary by location between diopside, enstatite, and ferrosilite, whereas amphiboles are mainly chlorine- and fluorine-rich magnesiohastingsite (Gates, 1995) and potassichastingsite (Lupulescu *et al.,* 2009).

Southeastern Shear Zone

The southeastern shear zone is located between Little Long Pond to the southwest and Lake Tiorati to the northeast. This zone contains the Hogencamp and Pine Swamp deposits. The mineralized vein that hosts both deposits is ~3 km long and ranges in thickness from 2 to 10 m at the mine locations to as little as one meter in the narrow zones that connect them. Country rock in this area includes metavolcanic and quartzofeldspathic gneiss, with diorite, calc-silicate, and marble locally.

Hogencamp Mine

The Hogencamp Mine lies in the southern part of the southeastern shear zone. The sheared wall rock is dominated by metavolcanic gneiss, with calc-silicate gneiss and marble locally. It is characterized by a series of 1 to 10 m wide horizontal and vertical mine shafts and open pit mines where the magnetite ore was extracted from the vein deposit. The vein is continuous along strike for about one km.

The bleached zone is characterized by fine-medium grained calcite (~15%) and scapolite (~15%), and the retrogression of pyroxene to amphibole (~45%), with phlogopite (<10%), albite (<10%), and minor fluorapatite locally (<5%) (Fig. 7 A). The layered vein is composed of 'bands' of individual fine-medium grained amphibole-, clinopyroxene-, and orthopyroxene-dominated assemblages, also containing calcite and phlogopite closest to the gradational bleached zone contact (Fig. 5). Layered vein banded assemblages Hv_1-Hv_4 are shown in Figure 5. Hv_1, the banded assemblage adjacent to the bleached zone, is composed dominantly of amphibole (~70%) and interstitial calcite (~15%) with minor clinopyroxene (<10%) and phlogopite (<5%). Farther within the vein, Hv_2 is mainly fine-medium grained amphibole (~60%) and clinopyroxene (~40%). Hv_3 is dominated by fine-medium amphibole (~45%) with lesser amounts of clinopyroxene (~35%) and orthopyroxene (~20%), whereas Hv_4 is dominated by medium grained orthopyroxene (~50%) and clinopyroxene (~30%) with lesser amounts of amphibole (~20%). The central massive vein is characterized by very coarse magnetite ore and coarse gangue minerals of clinopyroxene, amphibole, and biotite, cemented by interstitial calcite (Figs. 6 A; 7 B & C). Massive magnetite and coarse euhedral clinopyroxene crystallized first, followed by amphibole, biotite, and calcite. Table 1 summarizes the mineral assemblages associated with each of the deposits.

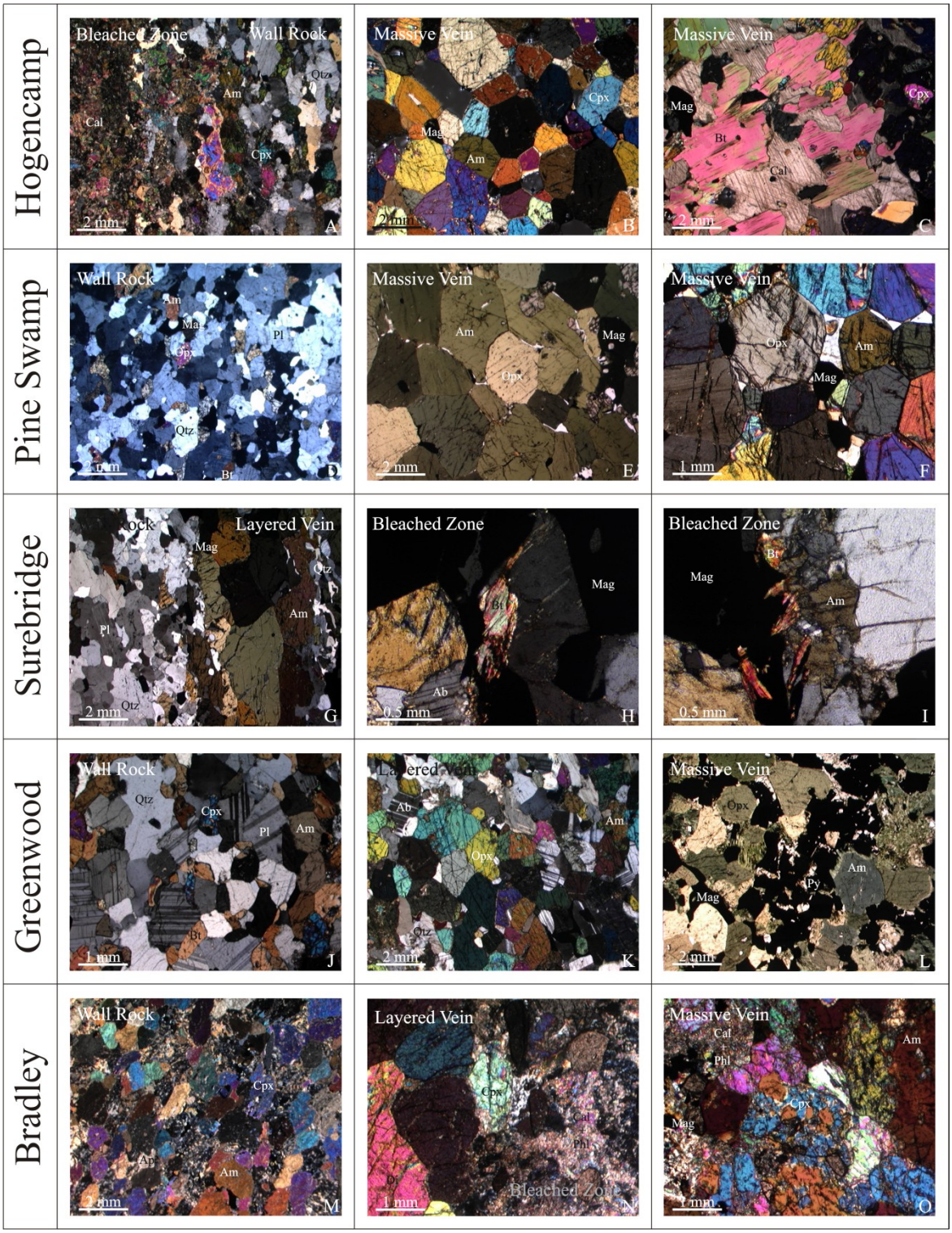

Figure 7. Photomicrographs of mineral assemblages from the magnetite deposits (crossed polarized light, E & L are ppl). (A) Wall rock/bleached zone contact, Hogencamp. (B & C) Massive vein material from the Hogencamp deposit, (B) Clinopyroxene-amphibole rich assemblage, (C) Calcite, biotite, clinopyroxene-rich assemblage. (D) Quartzofeldspathic wall rock from Pine Swamp. (E & F) Massive vein material from Pine Swamp showing amphibole, orthopyroxene,

magnetite-rich assemblages. (G) Wall rock, minor bleached zone, and layered vein contacts from the Surebridge deposit. (H & I) Bleached zone assemblages from Surebridge, containing (H) albite, biotite, and magnetite, and (I) sericite, amphibole and magnetite. (J) Wall rock from the Greenwood deposit, quartz, plagioclase, clinopyroxene, amphibole, and biotite. (K) Layered vein assemblage from Greenwood containing orthopyroxene, amphibole, albite, and quartz. (L) Massive vein from Greenwood, amphibole and orthopyroxene with interstitial pyrite, pyrrhotite, and magnetite. (M) Calc-silicate wall rock from Bradley. (N) Bleached zone/layered vein contact, bleached zone contains clinopyroxene, calcite and phlogopite. (O) Massive vein from Bradley containing clinopyroxene, amphibole, magnetite, calcite and phlogopite.

Table 1. Summary of mineral assemblages from the mineralized zones (lesser quantities).

Deposit	Wall Rock	Bleached Zone	Vein Deposit		Interstitial
			Layered	Massive	
Hogencamp	Metavolcanic Calc-silicate (Marble)	Calcite Scapolite Amphibole Phlogopite Albite (Flourapatite)	Amphibole Clinopyroxene Orthopyroxene (Calcite) (Phlogopite) (Biotite)	Magnetite Clinopyroxene Amphibole Biotite	Calcite
Pine Swamp	Quartzofeldspathic Metavolcanic	Amphibole (Scapolite) (Biotite) (Flourapatite)	Orthopyroxene Amphibole Quartz	Magnetite Orthopyroxene Amphibole	Pyrite Pyrrhotite
Surebridge	Quartzofeldspathic Metavolcanic	Amphibole Albite (Scapolite) (Sericite) (Magnetite)	Amphibole Orthopyroxene Magnetite Quartz	Magnetite Amphibole Orthopyroxene	Quartz Pyrite Pyrrhotite
Greenwood	Quartzofeldspathic	Not Present	Amphibole Orthopyroxene Albite Quartz Magnetite	Magnetite Amphibole Orthopyroxene	Quartz (Pyrite) (Pyrrhotite)
Bradley	Calc-silicate Marble	Diopside Scapolite Calcite Phlogopite	Clinopyroxene Phlogopite Calcite (Pyrite)	Magnetite Clinopyroxene Calcite	Calcite

Pine Swamp Mine

Pine Swamp Mine lies along strike about one kilometer to the northeast of the Hogencamp deposit. Pine Swamp is also characterized by a ~5 m wide horizontal mine shaft and ~10 m open pit mines. The vein that hosts the Pine Swamp deposit is about 500 m long, with minor semi-concordant veins in the northern extent of the deposit. This vein lies primarily in quartzofeldspathic gneiss and sulfide-bearing metavolcanic gneiss country rock, which varies between interlayered mafic and intermediate gneiss (Fig. 7 D).

The bleached zone is primarily defined by retrogression of medium grained pyroxene to amphibole (~80%), but it also contains minor amounts of fine-medium grained scapolite (<10%), biotite (~5%), and fluorapatite (<5%) locally. Medium-coarse grained orthopyroxene (~75%) and amphibole (~15%) dominate the narrow layered vein, with minor quartz (~10%). The massive vein contains the magnetite ore and gangue minerals of medium-coarse grained orthopyroxene (>80%) and lesser amounts of amphibole (<20%) (Fig. 7 E & F). The minerals in the massive vein are cemented by sulfide minerals, mainly pyrite and pyrrhotite. Large euhedral magnetite and sub-euhedral orthopyroxene crystallized first, followed by amphibole and interstitial sulfides.

Northwestern Shear Zone

The northwestern shear zone lies ~1 km to the northwest of the southeastern zone. This zone includes the Surebridge, Greenwood, and Bradley Mine deposits. The mineralized vein in the northwestern zone is continuous for ~4 km, and lies dominantly in quartzofeldspathic country rock, with metavolcanic, calc-silicate and marble locally.

Surebridge Mine

The Surebridge Mine is located at the southern end of the northwestern shear zone. The country rock is quartzofeldspathic gneiss, but it also contains sulfide-bearing

mafic metavolcanic gneiss. The Surebridge Mine is characterized by a ~5 m wide by ~30 m long central vein deposit, and two, narrower, sub-parallel secondary vein deposits. These secondary vein deposits are ~100 m to the east of the main vein. The much narrower veins are about ~2 to 3 m thick and up to ~20 m in length. They are observed as two, ~5 m deep pits, from which the iron ore was extracted.

The narrow bleached zone at Surebridge is composed primarily of fine grained amphibole (~75%) with minor albite (~15%), scapolite (~5%), and biotite locally (~5%) (Fig. 7 H & I). The layered vein sequence is only ~2 to 5 cm thick and composed dominantly of medium grained amphibole (~65%) with minor orthopyroxene (~15%), quartz (~15%), and magnetite (~5%) (Fig. 7 G). Massive vein minerals are coarse orthopyroxene and amphibole, and very-coarse magnetite in the core, with sulfides and some quartz as late interstitial cement.

Greenwood Mine

Greenwood Mine lies within the northwestern shear zone, between the Bradley deposit to the northeast and the Surebridge deposit to the southwest. It is contained within the quartzofeldspathic gneiss (Fig. 7 J) and the deposit is characterized by a series of sub-parallel veins. The main deposit ranges in thickness from 2 to 10 m and is ~30 to 40 m in length. The two sub-parallel veins are ~200 m to the south-east of the mine and are ~2 to 4 m thick and ~10 to 15 m long.

The bleached zone is absent and the vein is in direct contact with the wall rock. Wall rock contacts are sharp with the layered vein composed of medium grained amphibole (~60%), with minor fine grained orthopyroxene (~20%), albite (~10%), and quartz (~10%) (Figs. 8, 7 K). Coarse grained amphibole appears to exhibit a slight preferred orientation. The massive zone contains coarse magnetite and medium-coarse

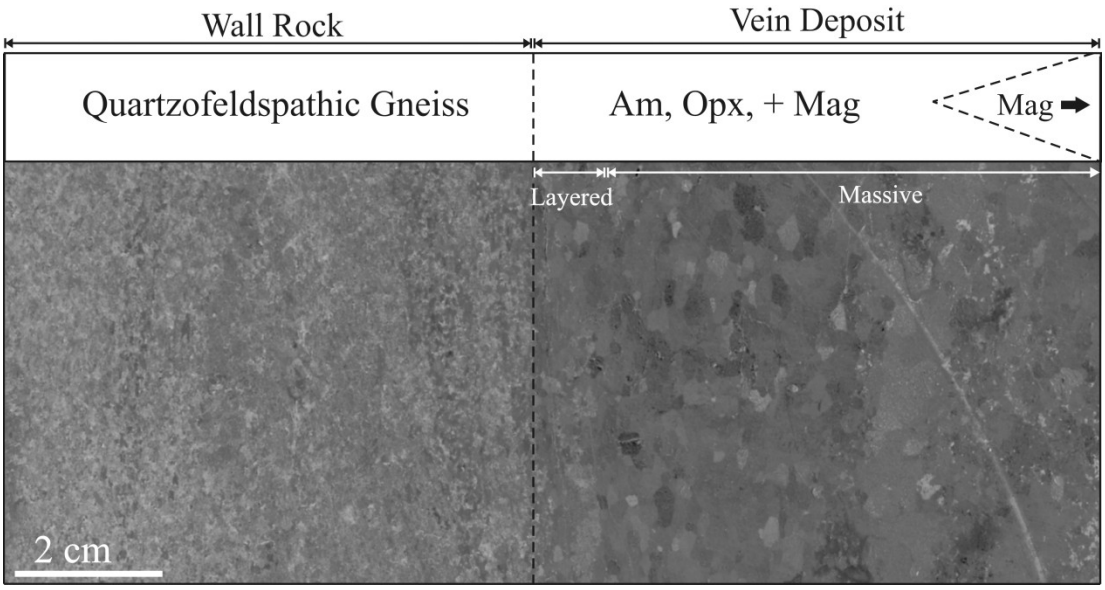

Figure 8. Greenwood deposit sample, showing mineral assemblages across the wall rock, vein deposit contact. No bleached zone is observed. Wall rock is interlayered mafic gneiss within the quartzofeldspathic unit.

grained amphibole and orthopyroxene-rich deposits cemented by interstitial quartz, and/or less commonly pyrite and pyrrhotite (Figs. 6 B & C, 7 L). Magnetite and sub-euhedral amphibole crystallized first, followed by orthopyroxene and interstitial quartz and sulfides.

Bradley Mine

Bradley Mine is the northern-most deposit in the northwestern shear zone. The Bradley deposit lies within calc-silicate country rock (Fig. 7, M) and hosts a ~5 to 10 m discontinuous body of diopside marble, composed of medium-coarse grained calcite, fine-medium diopside, and minor amounts of garnet locally. The vein deposit is ~200 m in length and varies in thickness from ~2 to 10 m.

The bleached zone is characterized dominantly by fine grained diopside (~70%), calcite (~15%), scapolite (~10%), and phlogopite (<5%). The layered vein is narrow and composed of fine-medium grained clinopyroxene (~85%), very fine grained phlogopite

(<10%), and minor amounts of fine grained calcite and sulfides, pyrite and pyrrhotite (<5%) (Fig. 7 N). Massive vein includes intergrowths of clinopyroxene and lesser amounts of amphibole and phlogopite cemented by calcite and the magnetite ore, in the core of the deposit (Fig. 7 O). Coarse magnetite and clinopyroxene was first to crystallize, followed by amphibole, phlogopite, and interstitial calcite.

GEOCHEMISTRY

Chemical Analysis

Twelve samples were collected for geochemical analysis across the wall rock-bleached zone boundary, from both shear zones. The samples are from various locations within each deposit, along the wall rock/vein contact. Several samples were analyzed and averaged from each deposit to account for inhomogeneity in the wall rock and bleached zones. Three samples each are from the Hogencamp (Hogencamp 1-3), Pine Swamp (Pine Swamp 1-3), and Bradley (Bradley 1-3) deposits, two are from the Surebridge (Surebridge 1-2) deposit, and one is from the Greenwood deposit (Greenwood 1). All samples were analyzed for major oxides, of which seven were also selected for trace element analysis (Tables A-1 – A-3). Samples of early layered vein assemblages were also analyzed from each deposit, as well as individual layers (Hv_1-Hv_4) from the layered vein in the Hogencamp deposit.

Initial sample preparation was conducted at Rutgers University, Newark, NJ. The samples were cut parallel to the mineralized 'bands' in cm-scale increments, isolating wall rock, 'bleached' zone, and layered vein deposit mineral assemblages. They were then pulverized into powder, using a jaw crusher. Three duplicates were independently prepared from each of the assemblages and analyzed separately. The chemical data were averaged for the three samples from the same band to eliminate minor variations in

composition. Subsequent sample preparation and analysis were conducted at Montclair State University, NJ, following procedures of Gorring *et al.,* (2004) (see Appendix-II). Samples were analyzed for bulk oxides and minor elements using a JY ULTIMA-C, multi-collector, ICP-OES (Appendix-II). Trace elements were analyzed using a Thermo-electron X-7 series quadrupole mass spectrometer (Appendix-II).

Southeastern Shear Zone

Bulk oxide chemical analyses from the southeastern shear zone are shown in Table 2. Wall rock samples from the Hogencamp deposit contain 57-68% silica, moderate amounts of aluminum (13-16%) and iron (4.5-8.5%), and varying amounts of potassium (1.6-5.3%), sodium (2.5-5.0%), calcium (3.8-9.9%), and magnesium (1.7-4.7%). Wall rock also contains minor amounts of titanium (0.4-1.1%), manganese (~0.1-0.2%), and phosphorus (~0.1-0.2%). Bleached zone assemblages from Hogencamp appear more intermediate to mafic in composition. Silica ranges from about 50-56%, aluminum between ~10-15%, whereas calcium (9.4-15.9%), iron (9.7-11.9%), and magnesium (3.8-7.2%) are all higher in the bleached zone. Sodium (0.9-4.4%), potassium (0.6-1.1%), and titanium (0.3-2.0%) appear variable in quantity.

Pine Swamp wall rock shows similar bulk chemistries to Hogencamp. Silica ranges from 56-69%, aluminum from about 12-16%, and iron varies from 6.4-8.3%. Sodium (4.2-5.0%), potassium (0.8-1.6%), titanium (0.7-0.9%), phosphorus (~0.1-0.2%), and manganese (<0.1%) appear relatively consistent. Larger differences in calcium (4.8-8.1%) and magnesium (2.3-4.8%) are also observed. Pine Swamp bleached zone shows large variations in silica (~53-67%), aluminum (10.5-15.5%), calcium (5.3-9.4%), and magnesium (2.4-6.2%). Smaller ranges in sodium (2.4-4.7%), potassium (1.2-2.9%), and

Table 2. Bulk oxide geochemical results (in wt%), southeastern shear zone (Table A-1).

Oxide	Hogencamp-1		Hogencamp-2		Hogencamp-3		Pine Swamp-1		Pine Swamp-2		Pine Swamp-3	
(wt%)	Wall	Bleached	Wall	Bleached	Wall	Bleached	Wall	Bleached	Wall	Bleached	Wall	Bleached
SiO_2	68.30	55.96	57.48	53.06	58.53	50.88	56.06	53.29	66.18	63.48	68.72	67.01
TiO_2	0.43	0.31	1.10	2.02	0.58	0.38	0.95	1.40	0.72	0.78	0.76	0.72
Al_2O_3	12.98	14.05	16.04	14.89	13.10	10.41	15.92	14.59	13.80	15.56	12.39	10.49
Fe_2O3	4.51	9.69	8.46	10.86	7.00	11.96	8.29	10.02	6.64	8.09	6.38	9.72
MnO	0.16	0.23	0.05	0.05	0.16	0.24	0.05	0.05	0.15	0.17	0.08	0.08
MgO	1.73	3.80	4.75	6.06	4.27	7.22	4.83	6.19	2.36	2.37	2.49	4.05
CaO	3.86	11.93	7.90	9.40	9.95	15.91	8.13	9.24	4.89	5.48	5.89	5.37
Na_2O	3.11	4.23	5.08	4.41	2.45	0.86	5.01	4.35	4.23	4.67	4.27	2.36
K_2O	5.34	0.57	1.63	1.12	5.33	1.05	1.34	1.17	1.61	2.47	0.84	2.95
P_2O_5	0.11	0.24	0.22	0.18	0.11	0.20	0.20	0.19	0.16	0.17	0.15	0.23
Total	100.53	101.03	102.71	102.06	101.46	99.10	100.78	100.50	100.74	103.24	101.96	102.97

titanium (0.7-1.4%) are also observed. Iron (8.1-10.0%), manganese (~0.1-0.2%), and phosphorus (~0.2%) vary slightly.

Trace element chemical analyses results from the southeastern shear zone are shown in the appendix (Table A-3), and REE spidergrams are shown in Figure 9. REE concentrations reflect the country rocks dominantly igneous protoliths. REE concentrations from the Hogencamp deposit wall rock and bleached zone show varying concentrations, though similar trends (Fig. 9 A & B). Bleached zone REE concentrations are only slightly enriched (Hogencamp-1) or slightly depleted (Hogencamp-2) compared to wall rock. Hogencamp-1 LREE and HREE are more enriched into the bleached zone compared to MREE, whereas Hogencamp-2, HREE and LREE are slightly more depleted, compared to MREE. Hogencamp-1 also has the highest concentration of REE in the southeastern zone, especially the LREE, also exhibiting the lowest values of the HREE.

Pine Swamp REE trends are comparatively more consistent between the wall rock and bleached zones (Fig. 9 C & D). Bleached zone REE are slightly depleted relative to wall rock in both analysis, and MREE remain the most consistent in concentration between wall rock and bleached zones. Pine Swamp-1 the MREE vary slightly, though

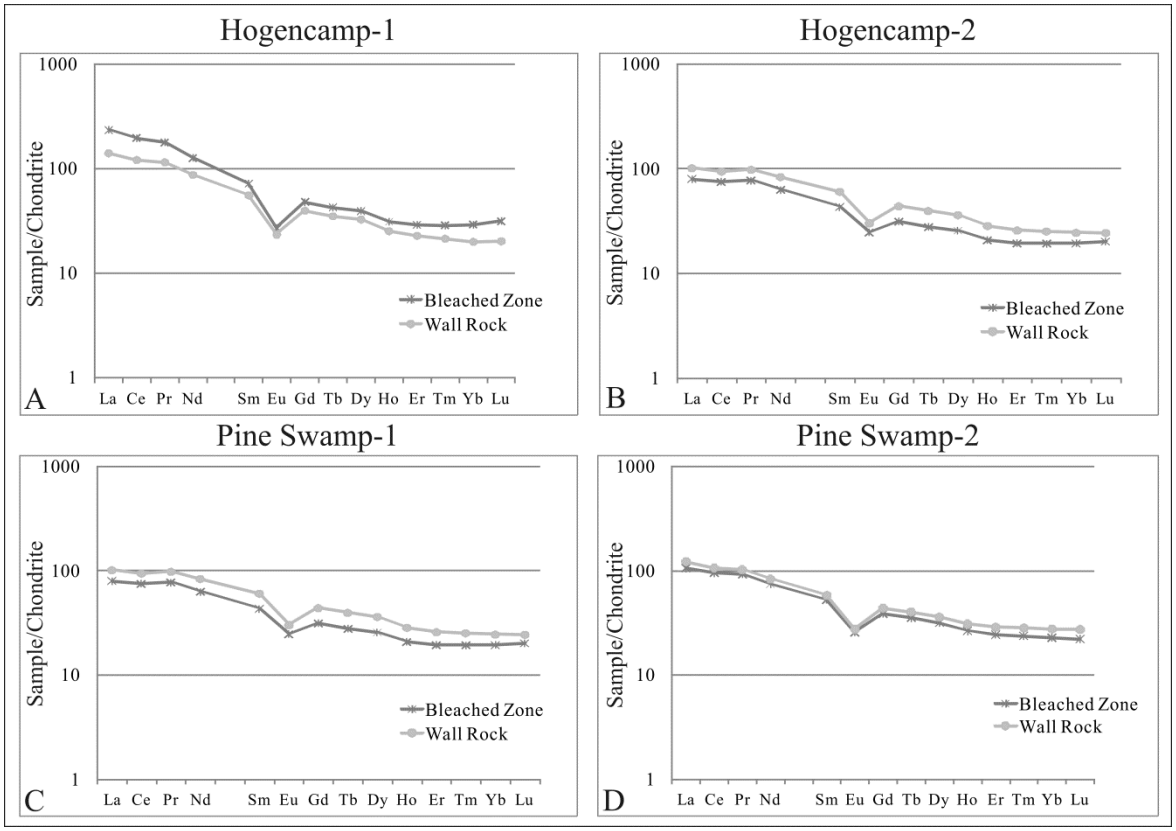

Figure 9. REE spidergrams from the southeastern shear zone, wall rock and bleached zones. Values are chondrite normalized (Anders & Grevesse, 1989)(Table A-3).

are more similar in concentration closer to the HREE and LREE. Pine Swamp-2 shows the least change in REE concentration between wall rock and bleached zone, with very minor differences in the HREE and LREE. All analysis from the southeastern shear zone exhibits a negative Eu anomaly.

Northwestern Shear Zone

Chemical analyses for the northwestern shear zone are shown in Table 3. Calc-silicate wall rock at the Bradley deposit is very high in calcium (19.8-21.8%), aluminum (~12-17%), and iron (8.3-12.7%), and low in silica (43.9-45.4%), sodium (0.8-1.2%), and potassium (0.2-0.7%). Magnesium (3.8-7.0%), titanium (0.1-2.2%), and phosphorus (~0.1-1.5%) all vary considerably. The bleached zone at Bradley is calcium- (~16-22%),

Table 3. Bulk oxide geochemical results (in wt%), northwestern shear zone (Table A-2).

Oxide	Bradley-1		Bradley-2		Bradley-3		Surebridge-1		Surebridge-2		Greenwood-1
(wt%)	Wall	Bleached	Wall	Bleached	Wall	Bleached	Wall	Bleached	Wall	Bleached	Wall
SiO_2	43.88	43.01	45.06	43.26	45.38	47.58	69.46	59.39	71.22	73.02	68.72
TiO_2	0.13	0.11	2.25	2.11	1.45	1.13	0.36	1.00	0.48	0.36	0.76
Al_2O_3	17.23	19.09	12.55	12.34	11.95	8.54	13.84	13.97	14.42	13.50	12.39
Fe_2O3	12.66	11.54	9.78	14.41	8.27	10.49	6.82	11.28	3.53	7.31	6.38
MnO	0.15	0.17	0.26	0.35	0.25	0.33	0.09	0.16	0.03	0.03	0.08
MgO	3.85	3.27	7.04	8.04	6.72	7.52	2.07	4.20	0.97	0.68	2.49
CaO	19.79	21.89	19.94	16.12	21.78	21.48	4.39	7.13	3.69	3.52	5.89
Na_2O	0.83	0.15	1.21	1.28	1.09	1.00	4.36	3.89	4.87	4.56	4.27
K_2O	0.18	0.07	0.74	1.25	0.22	0.33	0.79	0.95	0.67	0.55	0.84
P_2O_5	1.49	0.68	0.31	0.22	0.08	0.01	0.06	0.29	0.06	0.09	0.15
Total	100.19	99.98	99.15	99.37	97.18	98.42	102.24	102.25	99.95	103.62	101.96

aluminum- (8.5-19.1%), and iron- (10.5-14.4%) rich, and fairly low in silica (43.0-47.6%), potassium (~0.1-1.2%), sodium (~0.1-1.3%), and manganese (~0.2-0.3%). Magnesium (3.3-8.0%), titanium (0.1-2.1%), and phosphorus (<0.1-0.7%) also show the largest variations. Surebridge wall rock is sulfide-bearing quartzofeldspathic gneiss, characterized by about 70% silica, with significant amounts of aluminum (13.8-14.4%), calcium (3.7-4.4%), and sodium (4.4-4.9%), and lesser quantities of iron (3.5-6.8%), magnesium (~1-2%), and potassium (0.7-0.8%). Minor titanium (~0.4-0.5%), manganese (<0.1%), and phosphorus (<0.1%) are also present. The Surebridge bleached zone shows large variations in silica (59-73%), iron (7.3-11.3%), magnesium (0.7-4.2%), and calcium (3.5-7.1%). Aluminum (13.5-14.0%), sodium (3.9-4.6%), and potassium (~0.5-1.0%) appear relatively consistent among the samples. Wall rock at the Greenwood deposit is rich in silica (68.7%), aluminum (13.4%), calcium (5.9%), and sodium (4.3%). Moderate amounts of iron (6.4%) and magnesium (2.5%), and small amounts of potassium (0.8%) and titanium (~0.8%) are also present.

Trace element analyses from the northwestern shear zone are shown in the appendix (Table A-3), and REE spidergrams are shown in Figure 10. REE from the

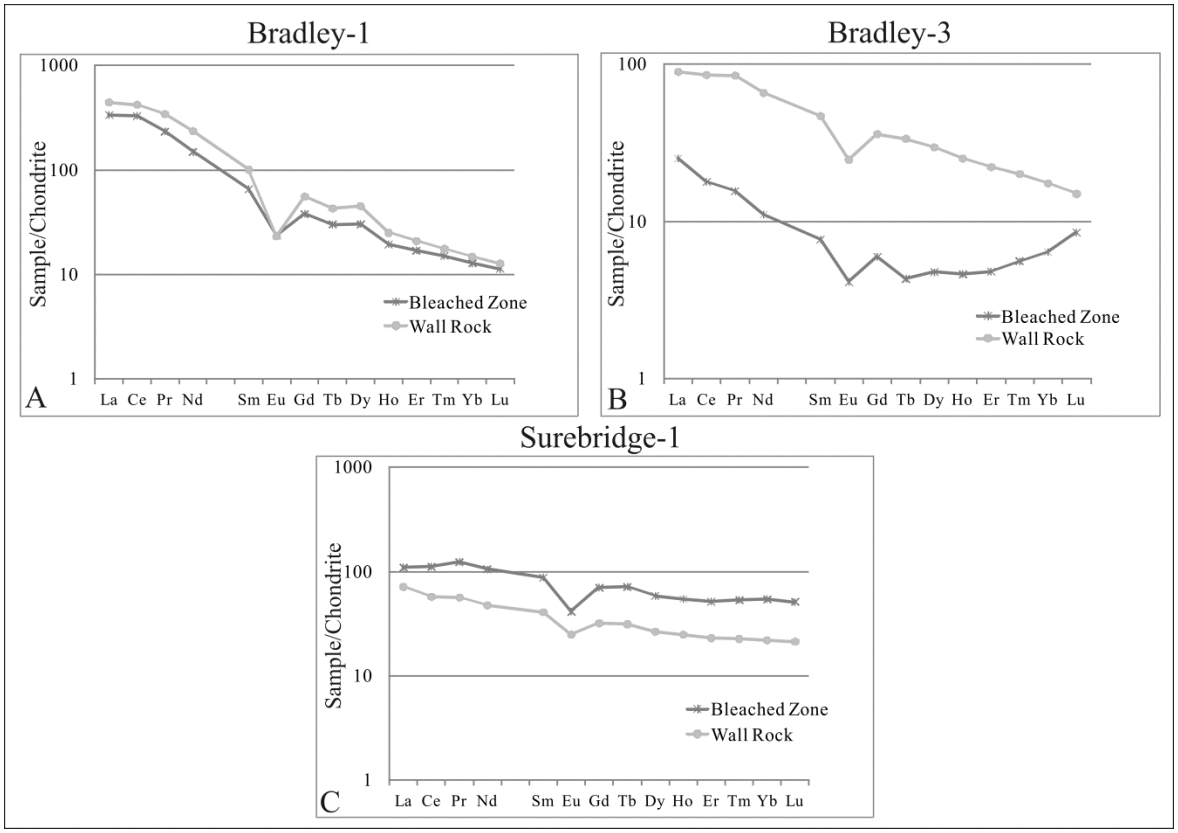

Figure 10. REE spidergrams from the northwestern shear zone, wall rock and bleached zones. Values are chondrite normalized (Anders & Grevesse, 1989)(Table A-3).

Bradley deposit wall rock and bleached zone show the greatest variation in concentrations (Fig. 10 A & B). Bradley-1 has the highest concentration of LREE in the northwestern shear zone, but it also has the lowest HREE values. Though slightly more depleted in MREE, Bradley-1 has the least change, showing only slightly lower REE concentrations into the bleached zone. REE concentrations between wall rock and bleached zone for Bradley-3 vary the greatest. Bleached zone REE are significantly depleted relative to wall rock. MREE are the most depleted into the bleached zone, however HREE and LREE are slightly less depleted from wall rock. REE concentrations from Surebridge-1 bleached zone are significantly enriched relative to wall rock (Fig. 10 C). LREE concentrations are the least enriched, though concentrations gradually rise into

the heavier REE's, and Eu appears the least mobile. In addition, all analysis display a negative Eu anomaly.

Vein Assemblages

The layered vein assemblages in contact with the bleached wall rock were analyzed for major elements (Table 4). Layered vein from the Pine Swamp deposit is iron-rich (31.6%) and low in silica (36.9%), with moderate amounts of calcium (9.1%), magnesium (9.1%), and aluminum (8.5%), and lesser amounts of sodium (1.6%) and potassium (1.4%), reflecting the amphibole/orthopyroxene rich assemblage. The Bradley deposit contains 44.8% silica, 17.3% iron, 12.8% aluminum, 10.2% calcium, 7.8% magnesium, 3.3% potassium, 2.3% titanium, and 2.0% sodium, consistent with the clinopyroxene, phlogopite, and calcite assemblage. Orthopyroxene and amphibole-rich layered vein from the Greenwood deposit is extremely iron-rich (35.4%), with moderate amounts of silica (37.3%), calcium (10.6%), aluminum (7.2%), and magnesium (7.1%), and lesser sodium (1.2%), potassium (1.1%), and titanium (0.4%). Layered vein from the Surebridge deposit is dominated by amphibole, orthopyroxene, and quartz, containing 43.4% silica, 24.9% iron, 10.3% aluminum, 9.7% calcium, and 7.8% magnesium, with lesser sodium (2.4%) and potassium (1.1%).

Bulk rock chemistries were also acquired in cm-scale bands across layered vein from the Hogencamp deposit (Table 5; Fig. 11). The locations of the bands are shown in Figure 5 (Hv_1-Hv_4). The bulk chemical composition resembles that of a mafic to ultramafic igneous rock (Table 5). Hv_1, composed dominantly of amphibole and calcite, with lesser amounts of phlogopite and clinopyroxene contains 48.0% silica, 17.6% calcium, 13.1% iron, 11.2% aluminum, 6.1% magnesium, and lesser amounts of sodium (1.9%), potassium (0.7%), and phosphorus (0.5%). Layer Hv_2, mainly diopside and

Table 4. Geochemical results for early layered vein assemblages.

Oxide (wt%)	Pine Swamp	Bradley	Greenwood	Surebridge
SiO_2	36.91	44.80	37.29	43.38
TiO_2	1.27	2.26	0.44	0.58
Al_2O_3	8.45	12.82	7.18	10.34
Fe_2O3	31.56	17.44	35.38	24.91
MnO	0.15	0.39	0.23	0.22
MgO	9.11	7.80	7.05	7.80
CaO	9.14	10.24	10.57	9.68
Na_2O	1.59	1.97	1.19	2.37
K_2O	1.36	3.34	1.06	1.07
P_2O_5	0.28	0.24	0.05	0.06
Total	99.82	101.30	100.44	100.42

amphibole, consists of 47.1% silica, 20.5% calcium, 14.0% iron, 8.6% magnesium, and 7.9% aluminum. Small amounts sodium (0.9%), phosphorus (0.8%), and potassium (0.3%) are also present. Hv_3 is dominated by amphibole with diopside and lesser amounts of orthopyroxene, containing 46.0% silica, 21.4% calcium, 11.7% magnesium, 12.1% iron, and 7.5% aluminum, with less phosphorus (1.3%), potassium (0.5%), and sodium (0.7%). Layer Hv_4 is mainly orthopyroxene and clinopyroxene with only minor amphibole, which contains 44.8% silica, 18.6% calcium, 13.3% magnesium, 11.6% iron, and 8.6% aluminum, and minor amounts of phosphorus (1.0%), potassium (1.1%), and sodium (0.9%).

General trends show a decrease in silica from 48.0-44.8% into the vein, whereas aluminum and sodium decrease progressively away from the wall (Hv_1) into the innermost analyzed layer (Hv_4), from 11.2-7.5% and 1.9-0.7%, respectively. Iron shows a small net loss from 13.1-11.6% inward, but magnesium increases from 6.1-13.3%. Potassium decreases close to the wall rock from 0.7-0.3%, but increases to 1.1% in Hv_4.

Table 5. Bulk oxide geochemical results of layered vein assemblages, from the Hogencamp deposit.

Oxide	Hogencamp Vein			
(wt%)	Hv_1	Hv_2	Hv_3	Hv_4
SiO_2	48.00	47.13	45.98	44.76
TiO_2	0.22	0.32	0.32	0.32
Al_2O_3	11.18	7.93	7.49	8.62
Fe_2O_3	13.06	13.95	12.10	11.59
MnO	0.25	0.27	0.20	0.17
MgO	6.08	8.59	11.73	13.25
CaO	17.58	20.45	21.42	18.58
Na_2O	1.86	0.91	0.65	0.91
K_2O	0.67	0.28	0.50	1.06
P_2O_5	0.49	0.79	1.30	1.02
Total	99.42	100.61	101.69	100.27

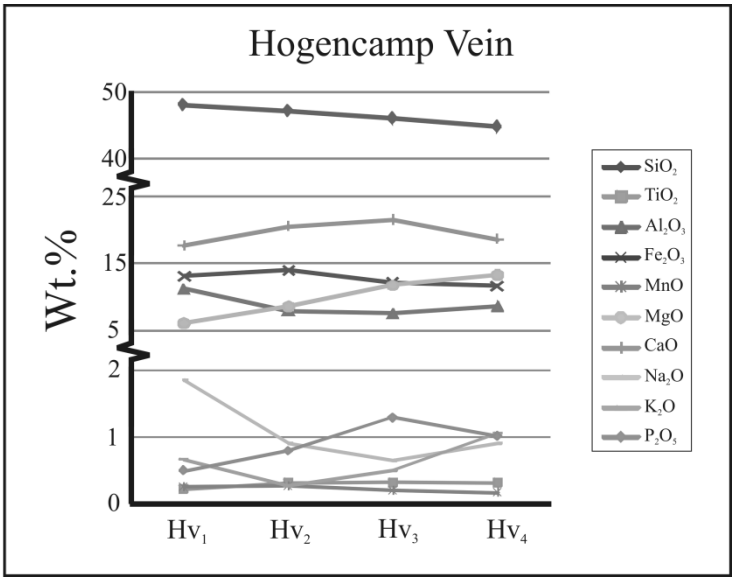

Figure 11. Bulk oxides of layered vein (Hv_1-Hv_4) from the Hogencamp deposit.

Similarly, calcium and phosphorus progressively increase but then decrease in the innermost layer (Hv_4) from 17.6-21.4% down to 18.6%, and 0.5-1.3% down to 1.0% respectively. Titanium remains relatively stable around 0.2-0.3% across all layers (Fig. 11).

Layered veins from the Hogencamp deposit were also analyzed for trace elements (Layers Hv_1-Hv_4; Table A-3), the REE spidergram is shown in Figure 12. The layered vein has a slight progressive increase in REE farther into the vein deposit from the wall rock contact. MREE are closest to the bleached zone in concentration, centered about Eu, whereas LREE and HREE progressively increase into the layered vein. Hv_1, layered vein closest to wall rock is slightly more enriched in HREE and LREE, relative to MREE, though REE trends approximate bleached zone trends, farther into the vein (Hv_4).

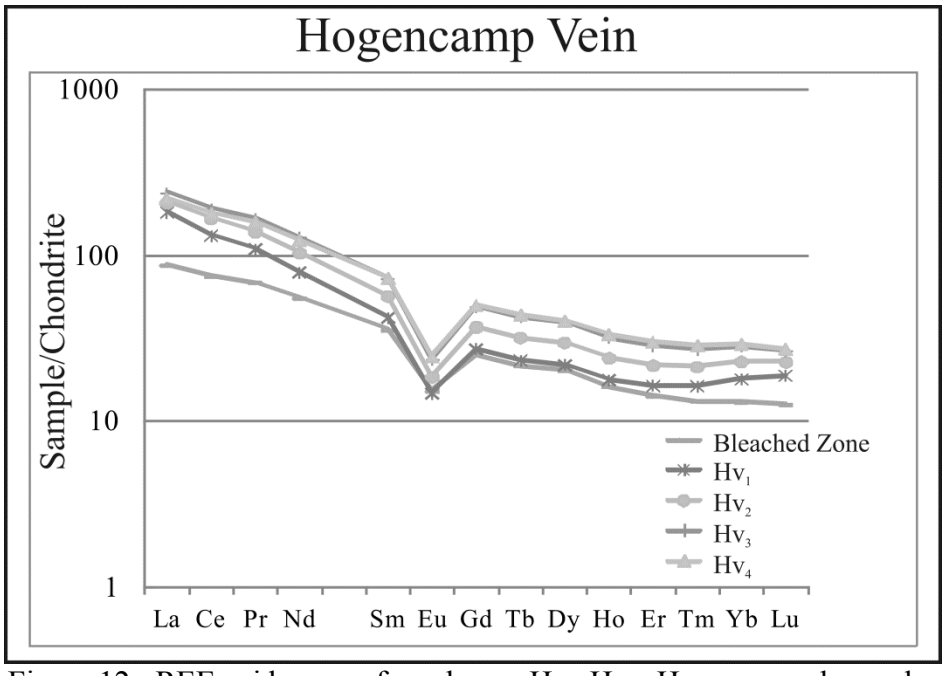

Figure 12. REE spidergram from layers Hv_1-Hv_4, Hogencamp layered vein. Values are chondrite normalized (Anders & Grevesse, 1989).

Mass Transfer

The geochemistry of the wall rock and bleached zone assemblages are compared to constrain elemental gains and losses into the metasomatic fluids within the zones from wall rock. To avoid misinterpretation from comparison of two sets of geochemical data the relationship between the composition and volume changes that accompany the processes must be considered (Gresens, 1967). To address this, Grant's Isocon analysis (1986), after Gresens (1967) equation for metasomatic alteration was applied to bulk oxide geochemistry results and density calculations (Tables 2 & 3). Sample densities were also directly measured (Table A-5). Constant aluminum or titanium was assumed during modeling. In addition, wall rock chemistries were averaged at each sampling location to reduce subtle variations due to compositional heterogeneity in the cm-scale samples of gneiss (Grant, 2005).

Geochemical and density data for wall rock and bleached zone were processed through Geoiso (Coelho, 2006), a program that calculates mass and volume changes during geological processes. Results are outputted as an overall rock mass and rock volume change, as well as changes in individual elemental species in mass and volume. The individual results from the isocon analysis (by percent volume change, Table A-4) were graphed for each sample from both shear zones. The amount of each oxide gained or lost was determined by multiplying the percentage volume change by the bulk rock composition for each oxide (Schleicher *et al.*, 2009). For this calculation only, the density differences between unaltered wall rock and bleached zones were considered to be negligible. The amount of each element gained or lost (in grams) per 100 grams of bulk wall rock was then established. The final mass transfer results ($\Delta g/100g$) were

averaged for each of the deposits to constrain 'overall' gains and losses into the bleached zone at each deposit.

Southeastern Shear Zone

Mass transfer modeling results (by volume) from the southeastern shear zone are shown in Figure 13. The volumetric changes for each oxide were multiplied by the analytical bulk-rock chemistry results of the wall rock, revealing the amount of each element gained or lost in grams per 100 grams of unaltered rock (Table 6). The bleached zone from the Hogencamp deposit reveals significant gains in iron (38-115%, 3.2-8.1g), magnesium (37-113%, 1.8-4.8g), calcium (28-185%, 2.2-10.1g), and manganese (8-97%, ~0.1-0.2g), with a loss of potassium (26-90%, up to 4.8g), and net losses in silica (up to 24.3%, 16.6g) and sodium (up to 55.6%, 1.4g) (Fig. 13 A-C), relative to the wall rock. The Pine Swamp deposit also shows significant gains in iron (12-60%, 0.8-3.8g), with net gains in potassium (up to 269%, 2.3g), calcium (up to 24%, 2.0g), and magnesium (up to 71%, 1.9g). Net losses in silica (up to 11%, 7.6g) and sodium (up to 42.4%, 1.8g) per 100 grams of wall rock are also observed (Fig. 13 D-F). Other elements show very small gains or losses.

Table 6. Calculated changes in volume (%), and calculated mass transfer (Δg/100g), from the wall rock into the bleached zone, southeastern shear zone.

	Hogencamp-1		Hogencamp-2		Hogencamp-3		Pine Swamp-1		Pine Swamp-2		Pine Swamp-3	
Oxide	Δ V	(g/100g)	Δ V	(g/100g)	Δ V	(g/100g)	Δ V	(g/100g)	Δ V	(g/100g)	Δ V	(g/100g)
SiO_2	-24.3%	-16.60	-0.6%	-0.34	9.4%	5.50	3.7%	2.07	-11.5%	-7.61	2.0%	1.37
TiO_2	-33.4%	-0.14	97.8%	1.08	-15.9%	-0.09	60.8%	0.58	0.0%	0.00	0.0%	0.00
Al_2O_3	0.0%	0.00	0.0%	0.00	0.0%	0.00	0.0%	0.00	4.1%	0.57	-11.4%	-1.41
Fe_2O_3	98.5%	4.44	38.3%	3.24	115.4%	8.08	31.9%	2.64	12.5%	0.83	60.2%	3.84
MnO	32.8%	0.05	7.7%	0.00	96.7%	0.15	9.1%	0.00	4.6%	0.01	5.7%	0.00
MgO	102.9%	1.78	37.4%	1.78	113.4%	4.84	39.8%	1.92	-7.3%	-0.17	71.0%	1.77
CaO	185.5%	7.16	28.2%	2.23	101.6%	10.10	24.0%	1.95	3.4%	0.17	-4.2%	-0.25
Na_2O	25.7%	0.80	-6.5%	-0.33	-55.6%	-1.36	-5.3%	-0.27	1.9%	0.08	-42.2%	-1.80
K_2O	-90.1%	-4.81	-26.0%	-0.42	-75.3%	-4.02	-4.7%	-0.06	41.6%	0.67	268.7%	2.25
P_2O_5	101.6%	0.11	-11.9%	-0.03	123.5%	0.14	3.7%	0.01	-1.9%	0.00	55.0%	0.08
Total	-5.4%	-7.21	10.82%	7.20	2.19%	23.34	7.16%	8.85	-8.96%	-5.47	10.91%	5.85

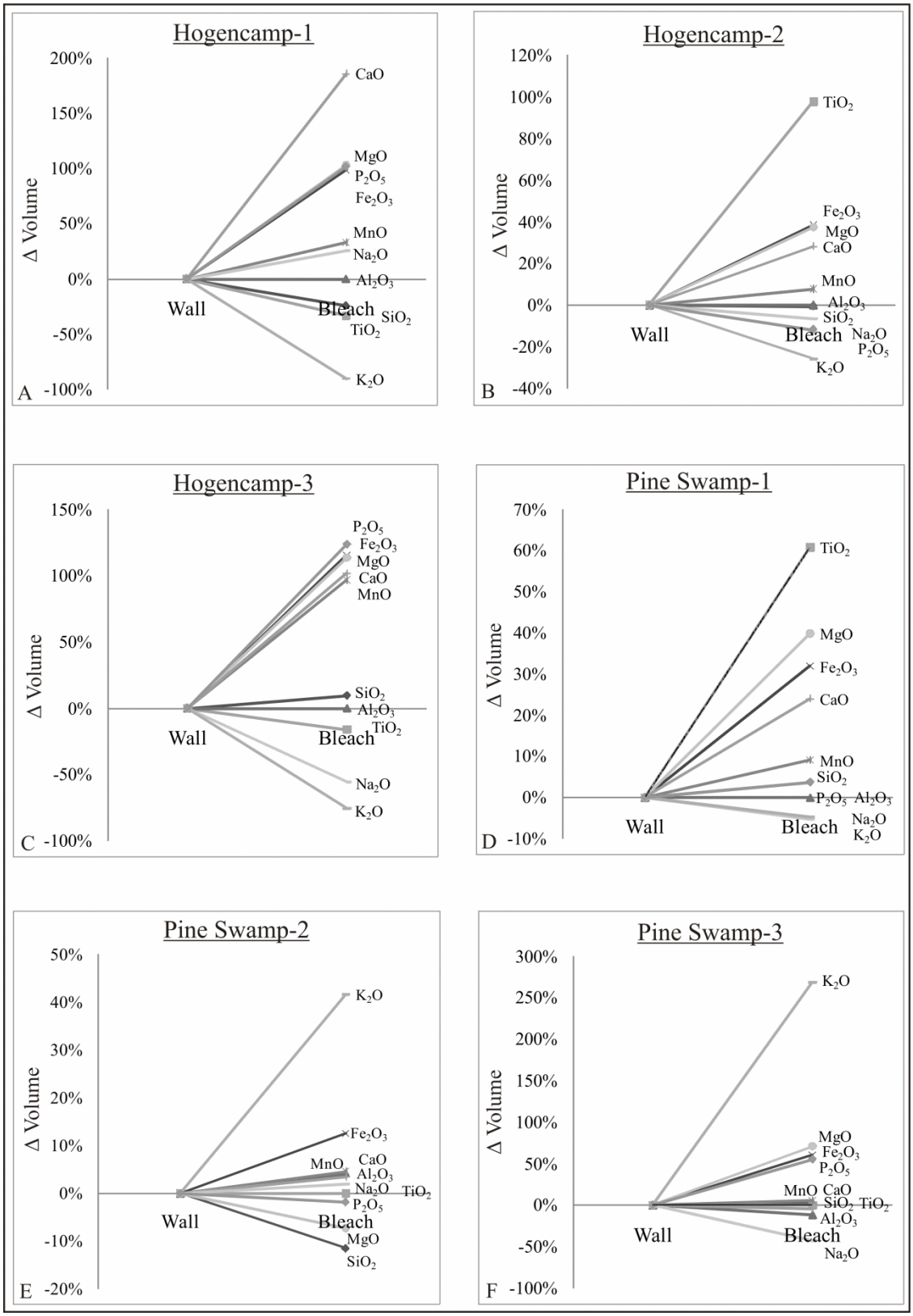

Figure 13. Volume percentage changes in oxides from the southeastern shear zone, across the wall rock-bleached zone boundary.

Rare earth element analysis results of the bleached zones were also normalized to wall rock concentrations and plotted on REE spidergrams (Fig. 14). Elements with values greater than 1 are enriched, whereas values less than 1 are depleted relative to wall rock. The Hogencamp deposit shows varying degrees of REE mass transfer (Fig. 14 A & B). Hogencamp-1 is the only bleached zone that gained REE, with significant gains in LREE and HREE, with lesser gains in MREE. However, Hogencamp-2 had moderate losses in all REE, with less of a loss in Ce, Eu, and Lu. The Pine Swamp deposit had small losses in all REE, slightly more so in Pine Swamp-1, with Eu being least mobilized and incorporated into the bleached zone (Fig. 14, C & D).

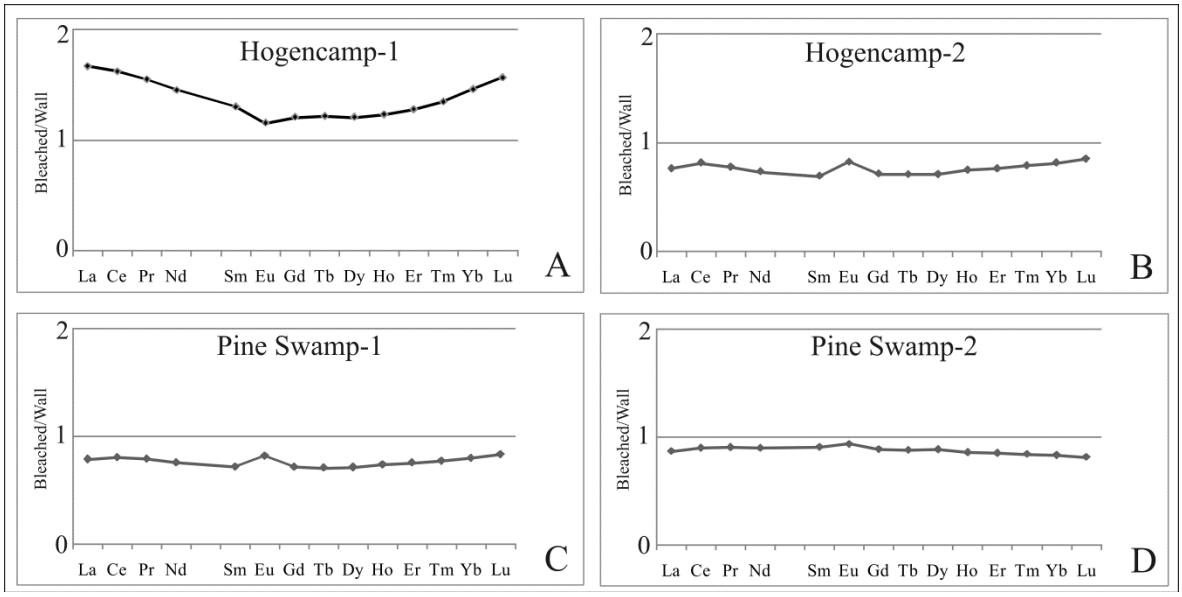

Figure 14. REE spidergram of southeastern shear zone, bleached zone normalized to wall rock. Values greater than 1 are enriched; less than 1 are depleted.

Northwestern Shear Zone

The mass transfer results from the northwestern shear zone are shown in Figure 15. The volumetric results from the isocon analysis from the northwestern shear zone were also multiplied by wall rock bulk chemistries to constrain elemental gains and losses in grams per 100 grams of unaltered wall rock (Table 7). Modeling of the Bradley

Table 7. Calculated changes in volume (%), and calculated mass transfer (Δg/100g), from the wall rock into the bleached zone, northwestern shear zone.

	Bradley-1		Bradley-2		Bradley-3		Surebridge-1		Surebridge-2	
Oxide	Δ V	(g/100g)	Δ V	(g/100g)	Δ V	(g/100g)	Δ V	(g/100g)	Δ V	(g/100g)
SiO_2	-2.9%	-1.27	-2.4%	-1.08	34.1%	15.47	-15.3%	-10.63	35.7%	25.42
TiO_2	-16.2%	-0.02	-4.8%	-0.11	0.0%	0.00	175.2%	0.63	0.0%	0.00
Al_2O_3	9.8%	1.69	0.0%	0.00	-8.6%	-1.03	0.0%	0.00	23.7%	3.42
Fe_2O_3	-9.7%	-1.23	49.7%	4.86	62.3%	5.15	63.9%	4.36	173.9%	6.14
MnO	12.3%	0.02	37.2%	0.10	69.4%	0.17	76.1%	0.07	37.1%	0.01
MgO	-15.9%	-0.61	16.1%	1.13	43.3%	2.91	101.0%	2.09	-8.1%	-0.08
CaO	9.6%	1.90	-17.7%	-3.53	26.1%	5.69	60.9%	2.67	26.4%	0.97
Na_2O	-82.1%	-0.68	7.8%	0.09	18.0%	0.20	-11.6%	-0.51	23.7%	1.16
K_2O	-61.5%	-0.11	69.9%	0.52	94.3%	0.20	19.1%	0.15	8.5%	0.06
P_2O_5	-54.8%	-0.82	-24.4%	-0.08	-83.8%	-0.07	378.8%	0.23	105.7%	0.06
Total	-2.57%	-1.14	43.36%	1.91	20.18%	28.70	-11.80%	-0.93	34.42%	37.17

deposit shows varying degrees of mass transfer. Overall gains in iron (up to 62%, 5.2g), manganese (12-69%, ~0.1g), silica (up to 34%, 15.5g), magnesium (up to 43%, 2.9g), calcium (up to 26%, 5.7g), and potassium (up to 94%, 0.5g), and a net loss of sodium (up to 82%, 0.7g), are observed relative to wall rock (Fig. 15 A-C). The Surebridge deposit shows the largest gains in mass. Modeling reveals significant gains in iron (64-174%, 4.4-6.1g), calcium (26-61%, 1.0-2.7g), potassium (9-19%, 0.1-0.2g), and phosphorus (106-379%, ~0.1-0.2g), with net gains in silica (up to 36%, 25.4g), magnesium (up to 101%, 2.1g), and sodium (up to 24%, 1.2g) relative to 100g of unaltered wall rock (Fig. 15 D-E).

Normalized bleached zone to wall rock REE spidergrams for the northwestern shear zone are shown in Figure 16. Analysis of the Bradley deposit shows losses in all REE into the bleached zone. Bradley-1 had moderate losses in all REE, less so the HREE, however Eu had no change. Bradley-3 had large losses of all REE into the bleached zone, though less so in the heaviest REE. Surebridge-1 was the only bleached

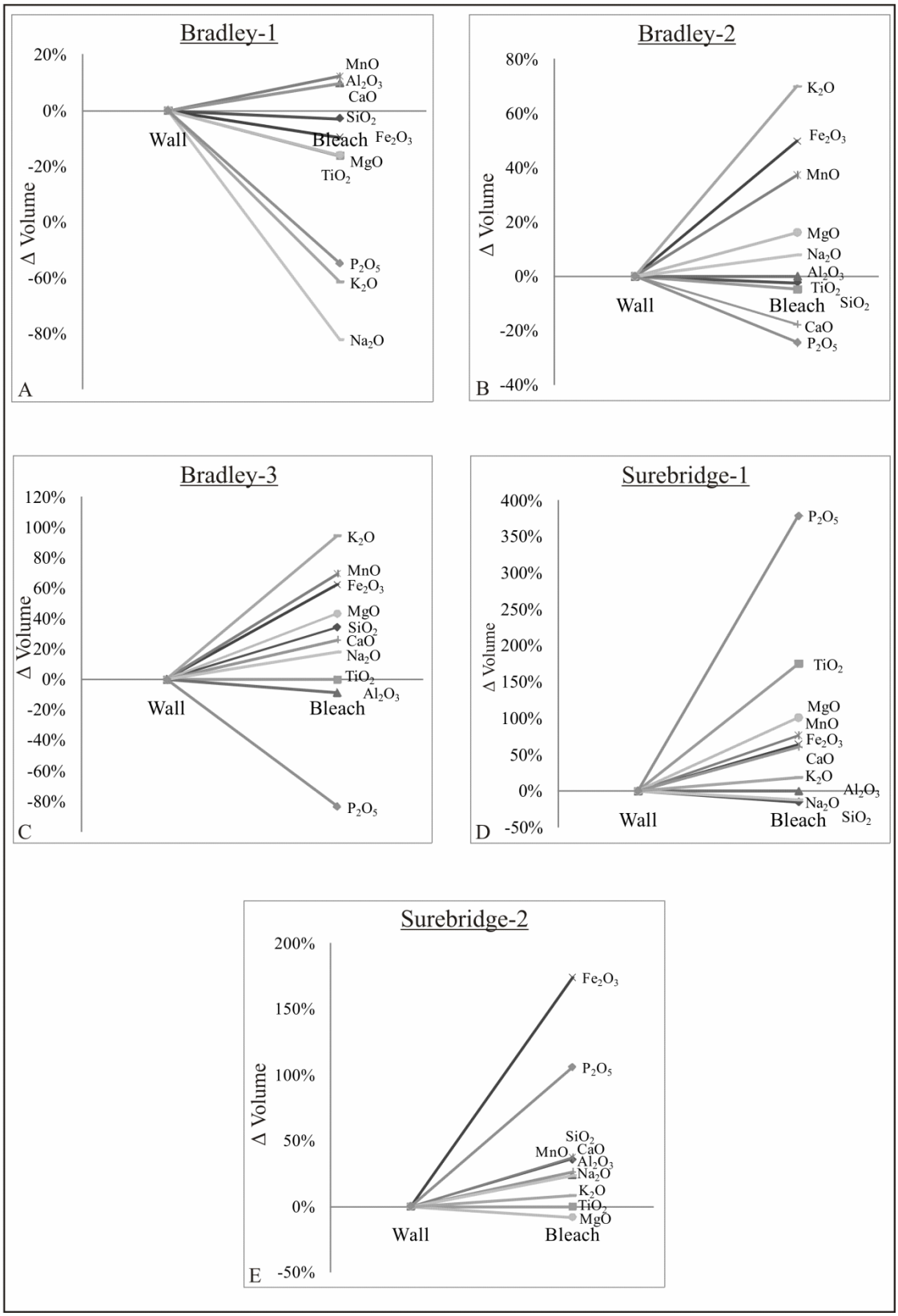

Figure 15. Volume percentage changes in oxides from the northwestern shear zone, across the wall rock-bleached zone boundary.

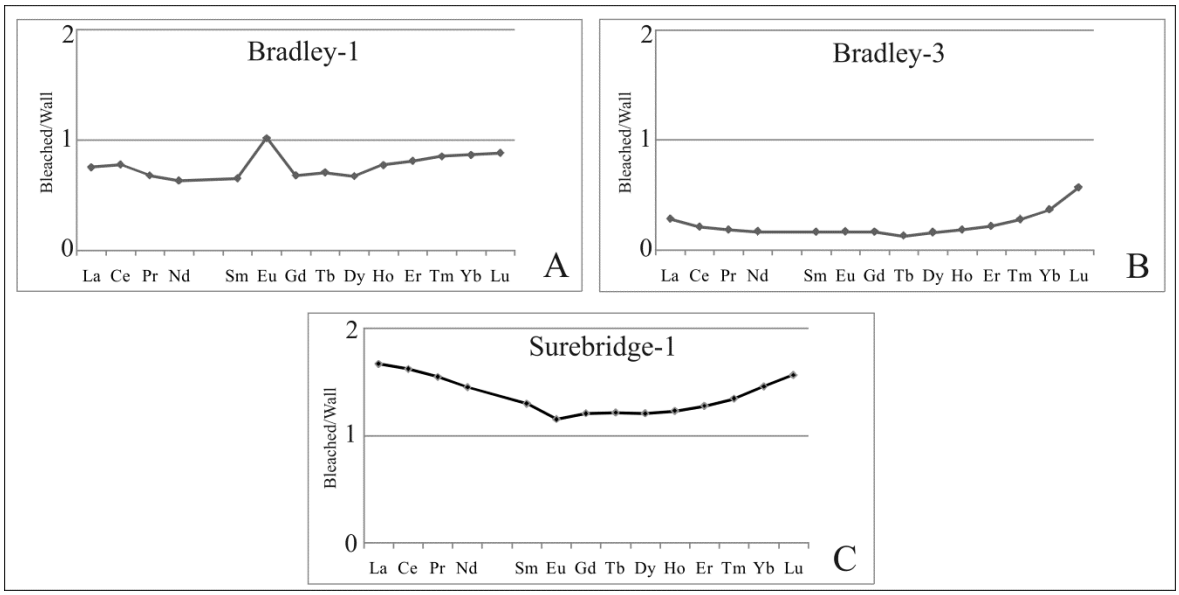

Figure 16. REE spidergram of northwestern shear zone, bleached zone normalized to wall rock. Values greater than 1 are enriched; less than 1 are depleted.

zone to gain REE in the northwestern shear zone. Large gains in both LREE and HREE occurred, with moderate gains in MREE relative to wall rock (Fig. 16 C).

Element Mobility

Bulk wall rock geochemistry (wt%) was plotted verses overall gains and losses (Δg/100g) into the bleached zone (Fig. 17). Silica varies, though the greatest changes in mass are concentrated towards the most silica-rich wall rock. Titanium and aluminum were generally considered immobile, though minor gains or losses occurred in calc-silicate rock from Bradley and quartzofeldspathic rock from Surebridge. Iron was gained in all but one bleached zone, regardless of country rock, and the largest gains were in iron-rich country rock. The only bleached zone not to gain iron, from the Bradley deposit, had the highest abundance in country rock (~13%), showing a minor loss of ~1.5g/100g from wall rock relative to the bleached zone. Manganese was gained in all the bleached zones, regardless of wall rock composition. Magnesium varies, though the largest gains in the bleached zone are observed in country rock which has magnesium in

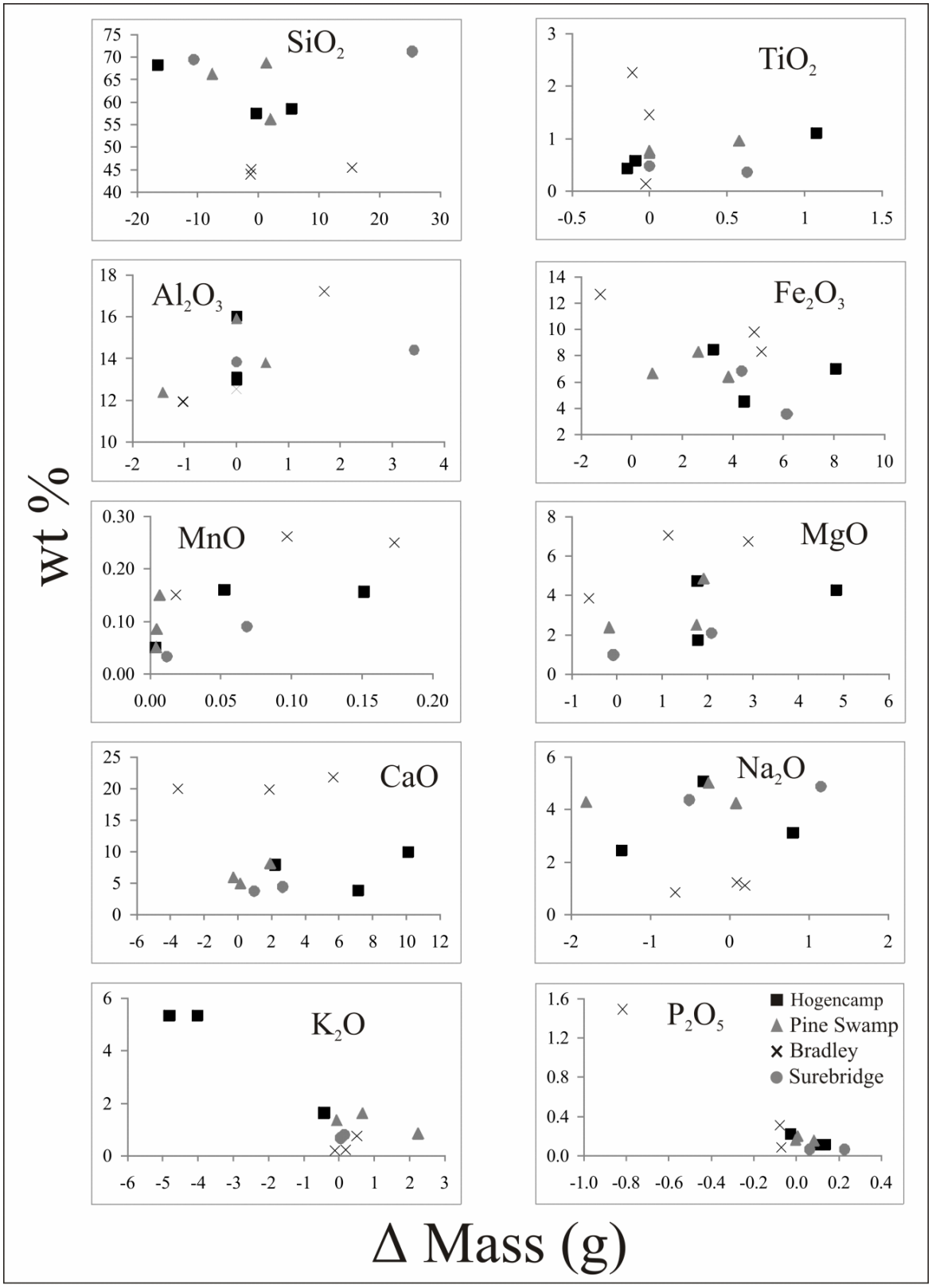

Figure 17. Wall rock bulk oxides verses calculated mass transfer (Δg/100g wall rock).

the highest abundances (~4-7%), with minor gains or losses from wall rock with lower concentrations. Calcium was very mobile, showing mostly gains into the bleached zone, the largest of which are found in deposits in/or adjacent to calc-silicate and/or marble country rock (*i.e.* Hogencamp and Bradley). Sodium resembles silica, but has the largest variance, with the greatest variations in the most sodium-rich wall rock. Potassium varies only slightly with low concentrations and had only minor gains in the Pine Swamp and Bradley deposits. Potassium-rich wall rock from Hogencamp (~5%) however, had a significant loss into the bleached zone (~4-5g/100g). Phosphorus also varies only slightly in low concentrations, although phosphorus-rich country rock from Bradley (~1.5%) had a relatively large loss into the bleached zone (~0.8g/100g). These results are also used to model a primordial fluid composition (see discussion).

Rare earth elements were also mobilized during bleached zone alteration. REE from the Hogencamp deposit were the most mobilized in the southeastern shear zone, with minor gains or losses of all REE in the bleached zone (Fig. 14). The Pine Swamp deposit had only small losses, but in all the REE. In both deposits, MREE are least mobile, showing the least amount of change from wall rock values. REE from the northwestern shear zone were more mobilized, showing greater variation from wall rock values (Fig. 16). Calc-silicate wall rock from the Bradley deposit is significantly depleted in REE into the bleached zone, with a very minor gain in Eu in one analysis. The Surebridge deposit is the only bleached zone to gain REE in the northwestern shear zone, the least mobile elements centered about the MREE. LREE and HREE were the most mobilized during mass transfer, and MREE were less likely to be buffered into solution. Eu appears the most stable, being the most consistent between wall rocks and bleached zones.

Averages

Averages of all analyzed wall rock and mass transfer calculations were compiled to better constrain the overall net gains and losses associated with each deposit, and to account for inhomogeneity in wall rock and bleached zones (Table 8, Figs. 18 & 19). Average metavolcanic wall rock compositions from the Hogencamp deposit resemble an intermediate igneous rock, containing 61.4% silica, 14.0% aluminum, 7.2% calcium, 6.7% iron, 4.1% potassium, and 3.6% magnesium and sodium. The bleached zone had significant gains in calcium (6.5g), iron (~5.3g), and magnesium (2.8g), with lesser gains in titanium (~0.3g), manganese (<0.1g), and phosphorus (<0.1g). Large losses in silica (3.8g) and potassium (3.1g), and a lesser extent sodium (0.3g) are also observed. On average, about 7.8 grams of material was added to the bleached zone, relative to 100 grams of wall rock. Averaged wall rock from the Pine Swamp deposit contains 63.7% silica, 14% aluminum, 7.1% iron, 6.3% calcium, 4.5% sodium, 3.2% magnesium, and 1.3% potassium. On average, the Pine Swamp deposit gained iron (2.4g), magnesium (~1.2g), potassium (~1.0g), and calcium (0.6g), with minor gains in titanium (~0.2g), manganese (<0.1g), and phosphorus (<0.1g). Silica (~1.4g), sodium (~0.7g), and minor aluminum (~0.3g) are all lost, for an overall net gain of about 3.1 grams per 100 grams of wall rock.

Averaged calc-silicate wall rock from the Bradley deposit contains 44.8% silica, 20.5% calcium, 13.9% aluminum, 10.2% iron, 5.9% magnesium, 1% sodium, and 0.4% potassium. Significant gains in silica (~4.4g), iron (2.9g), calcium (~1.4g), and magnesium (1.1g), and smaller gains in aluminum (0.2g), potassium (0.2g), and manganese (0.1g) are observed in the bleached zone. Minor phosphorus (0.3g), sodium (0.1g), and titanium (<0.1g) are lost for an overall net gain of about 9.8 grams per 100

Table 8. Average wall rock bulk oxides and calculated mass transfer into the bleached zone.

Oxide	Hogencamp Mine		Pine Swamp Mine		Bradley Mine		Surebridge Mine	
(wt%)	Wall	(Δg/100g)	Wall	(Δg/100g)	Wall	(Δg/100g)	Wall	(Δg/100g)
SiO_2	61.44	-3.81	63.65	-1.39	44.77	4.37	70.34	7.40
TiO_2	0.70	0.28	0.81	0.19	1.28	-0.04	0.42	0.32
Al_2O_3	14.04	0.00	14.04	-0.28	13.91	0.22	14.13	1.71
Fe_2O3	6.66	5.25	7.10	2.44	10.24	2.93	5.17	5.25
MnO	0.12	0.07	0.09	0.01	0.22	0.10	0.06	0.04
MgO	3.58	2.80	3.23	1.17	5.87	1.14	1.52	1.01
CaO	7.24	6.50	6.30	0.62	20.51	1.35	4.04	1.82
Na_2O	3.55	-0.30	4.50	-0.66	1.04	-0.13	4.62	0.32
K_2O	4.10	-3.08	1.26	0.95	0.38	0.20	0.73	0.10
P_2O_5	0.15	0.07	0.17	0.03	0.63	-0.32	0.06	0.15
Total	101.57	7.78g	101.16	3.08g	98.84	9.82g	101.09	18.12g

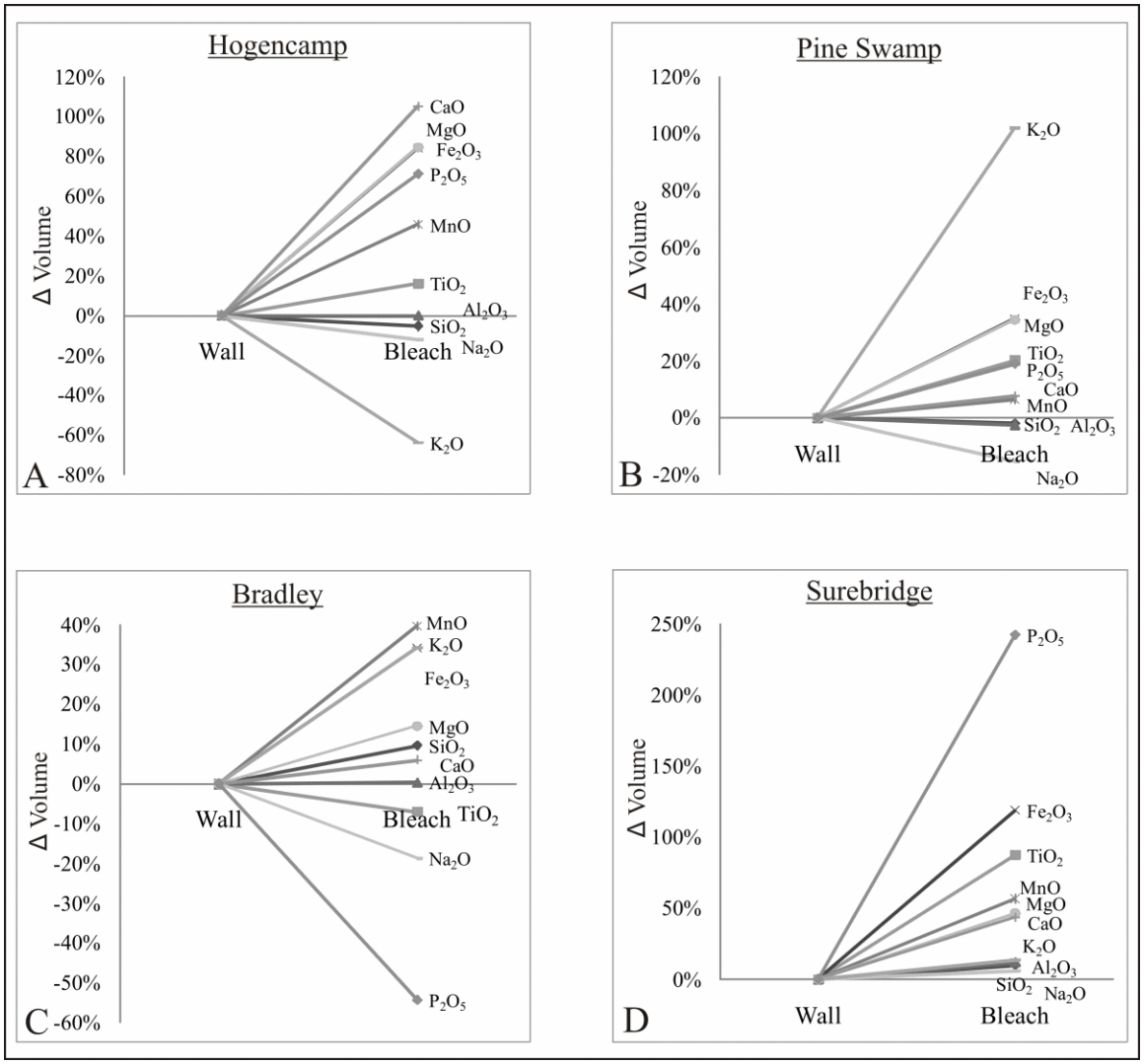

Figure 18. Average volume percentage change in oxides from the southeastern (A & B) and northwestern (C & D) shear zones, across the wall rock-bleached zone boundary.

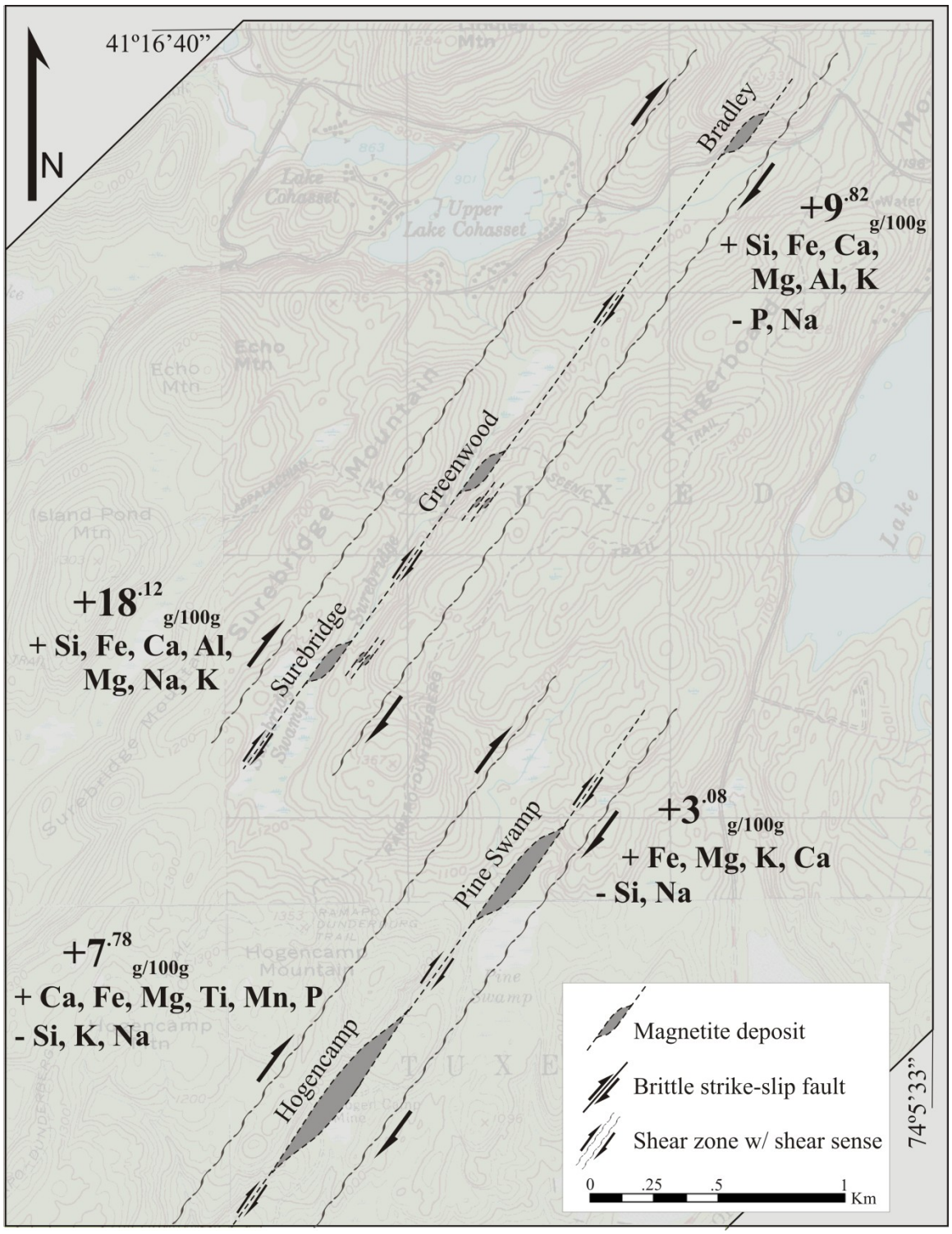

Figure 19. Map showing average mass transfer results (Δg/100g), and individual oxide gains and losses into the bleached zones.

grams of wall rock. Quartzofeldspathic and metavolcanic wall rock from the Surebridge deposit appears the most silica-rich with 70.3% silica, 14.1% aluminum, 5.2% iron, 4.6% sodium, 4% calcium, 1.5% magnesium, and 0.7% potassium on average. The Surebridge deposit shows average gains in all elements, including considerable amounts of silica (7.4g), iron (~5.3g), calcium (1.8g), aluminum (1.7g), and magnesium (1.0g). Lesser amounts of sodium (0.3g), titanium (0.3g), phosphorus (~0.2g), potassium (0.1g), and manganese (<0.1g) were also gained. The Surebridge deposit also shows the largest overall gain, with about 18.1 grams of material added to alter the bleached zone from the wall rock (Fig. 19).

Fluid Flux

Fluid Fluxes responsible for wall rock alteration were calculated using the methods of Ferry and Dipple (1991) and Dipple and Ferry (1992), based on the mobility of silica using the average mass transfer results. Pressures between 7-8 kbars and ~700°C were assumed, associated with the upper limits of brittle deformation and the waning stages of granulite facies metamorphism of the Highlands (see Discussion). Fluid fluxes all varied within an order of magnitude, 5.3×10^5 cm^3/cm^2 to 3.5×10^6 cm^3/cm^2 in the southeastern zone, and from 2.1×10^6 cm^3/cm^2 to 6.6×10^6 cm^3/cm^2 in the northwestern zone. Fluxes for Hogencamp were calculated as 1.5×10^6 cm^3/cm^2 to 3.5×10^6 cm^3/cm^2 between wall rock and bleached zone. Fluid flux from the Pine Swamp deposit varied slightly more, from 5.3×10^5 cm^3/cm^2 to 1.2×10^6 cm^3/cm^2.

In the northwestern zone, fluid fluxes for the Surebridge deposit were calculated between 2.9×10^6 cm^3/cm^2 to 6.6×10^6 cm^3/cm^2 and between 2.1×10^6 to 4.7×10^6 cm^3/cm^2 for the Bradley deposit. The calculated fluxes fall within the lower limits of fluid flux ranges required for major element metasomatism (10^6 to 10^8 cm^3/cm^2), enough

for dramatic alteration of wall rock (Ferry and Dipple, 1991). Independently calculated fluid fluxes for each sample also varied within an order of magnitude of the fluxes calculated from the averages of each deposit.

Calculated fluid fluxes appear to have a direct linear correlation between the volume of flux, and overall mass transfer, where overall gains in mass increased with increasing fluid flux (Fig. 20). The Surebridge bleached zone has the highest values of calculated flux, ranging up to 6.6 x 10^6 cm^3/cm^2, and on average gained up to ~18.1g relative to 100g of unaltered wall rock. The next highest calculated fluid flux, from the Bradley bleached zone, ranged up to 4.7 x 10^6 cm^3/cm^2, and gained up to ~9.8g of mass. Fluid fluxes calculated for Hogencamp bleached zone alteration ranged up to 3.5 x 10^6 cm^3/cm^2, on average gaining about 7.8g of mass to alter 100g of wall rock. The Pine Swamp bleached zone has the lowest values of calculated fluid flux, ranging up to 1.2 x 10^6 cm^3/cm^2, also with the smallest gains in mass, ~3.1g relative to 100g of unaltered wall rock. Fluid fluxes at the Surebridge deposit must not have been sufficient enough to allow for fluid infiltration of the wall rocks and bleached zone alteration. Fluxes must have been below the threshold defined by Dipple and Ferry (1991), such that major

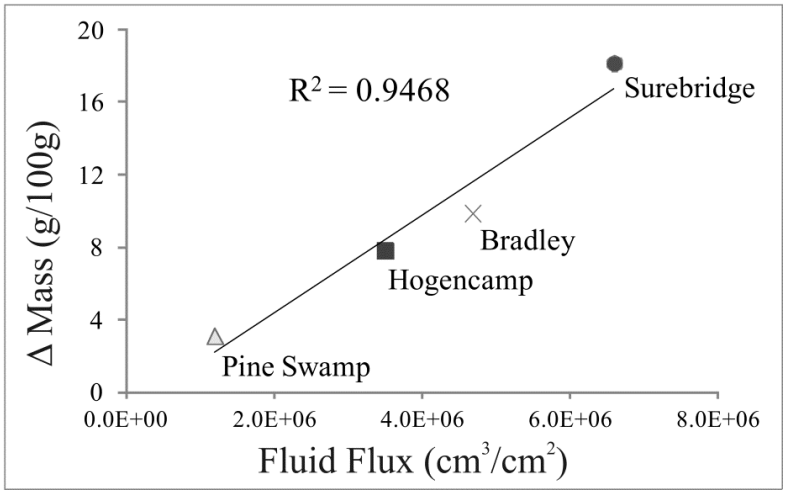

Figure 20. Average bleached zone mass gains versus calculated fluid flux from the deposits modeled.

element metasomatism did not occur here. Additionally, the linear relationship between mass transfer and fluid flux validates the flux calculations, using the mobility of silica, which in turn represents the general behavior of all elements in the system during bleached zone alteration, the more fluid flux, the greater the mass transfer.

DISCUSSION

Dextral Fault System

Dextral strike-slip movement occurred around 1,008 - 924 Ma (Gates and Krol, 1998), during a period of uplift and unroofing. Total offset was upwards of hundreds of kilometers, as thick anastomosing zones of mylonite formed (Gates *et al.*, 2006). Strike-slip shearing continued during decreasing temperature of the country rock, resulting in the shear zones crossing the brittle-ductile transition and becoming dilational (Gates *et al.*, 2003). Right step-over, pull-apart structures or 'dilational jogs' (Sibson, 1985) developed oblique to the local shear plane and linked (at least) two en-echelon faults parallel to it (Fig. 21).

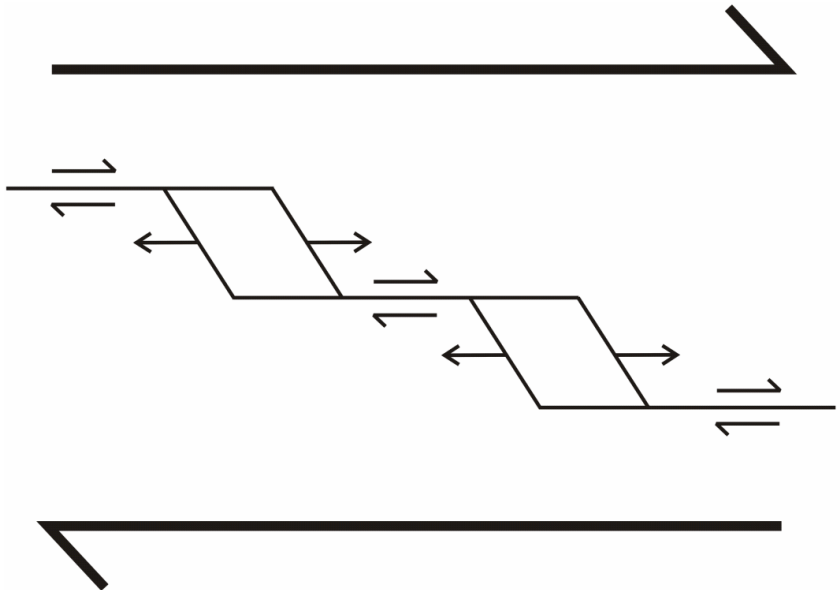

Figure 21. Schematic diagram illustrating dilation parallel to, and vein oblique to the shear plane, creating right step-overs in a dextral strike-slip shear zone (modified after McCaig, 1987).

The dilational faults formed within the brittle/ductile transition zone, such that brittle faulting overprinted ductile deformational fabrics. As temperature of the country rock began to fall, the segments of the fault began to dilate and fill with metamorphic fluids. High fluid pressure and relatively lower temperature of the surrounding country rock preserved sufficient rigidity, and allowed the dilational structures to remain open as they became fluid filled cavities, not empty void spaces, which cannot exist at depth. The faults than served as conduits for large volumes of the metamorphic/hydrothermal fluids.

The veins formed through the transport of ions in aqueous solutions from a source region to the fault zones. Below 10 km, open pore spaces are closed by compaction and recrystalization, and motion of fluids along fractures or grain boundarys are the only ways that fluids can migrate in the deeper crust (Winter, 2001). Dispersed iron from ferromagnesian minerals in the country rock, and possibly other deeper crustal sources, was collected and concentrated into these aqueous solutions and they migrated towards the dilational sections of the fault zones which were areas of relatively lower pressure. The faults had a pronounced effect on 'capture' of fluid from the regional system, which resulted in substantial fluid focusing (Oliver, 2001). In this way, the regional-scale hydrothermal system channeled fluids into the km-scale ductile shear zones, where magnetite mineralization could eventually take place.

Seismic pumping

The fluids flushed into the dilational segments of the faults through pressure gradients. The lower pressures in the dilational zones induced an inwards migration of fluid from the surrounding crust (Sibson *et al.*, 1975). The decrease in fluid pressure (P_{Fluid}), from lithostatic towards partially hydrostatic in these areas, decreased the solubility of the ions in the fluids and they altered and precipitated minerals on the vein

walls. Filled with these fluids, we suggest that seismic events along the faults further opened the dilational zones. The individual earthquakes acted as a pumping mechanism (Sibson *et al.*, 1975), moving significant quantities of mineralizing fluid rapidly from one dilational segment to another. Hydrothermal mineralization may have resulted from each seismically induced fluid pulse (Sibson *et al.*, 1975), and the mechanism also provides an explanation for the early layered textures of the vein deposit. Without repeated movement and dilation, vein minerals would eventually seal the fault zone and metasomatism would stop (Hagner *et al.*, 1963). Massive assemblages formed when the faults dilated much farther and crystallization was no longer limited to the vein walls.

We also speculate that seismically induced dilatancy pumping events occurred on two scales. On the small scale, little displacement and dilation occurred. Any fluids introduced and trapped within the fault zones behaved as a relatively closed system, in that, the fluids were internally buffered to local wall rock chemistry, there is no exchange with exterior fluids, and no further large volumes of fluids with a composition controlled by an outside reservoir are introduced. Fluid composition was dependent on the local wall rock and mixing of the fluids was limited to within the fault zones. On the large scale however, much greater and more rapid displacement and dilation occurred along the faults. With larger dilational zones and greater movement along the fault, the system behaved more as an open system, allowing large volumes of fluids to be introduced from outside reservoirs. Eventually, mineralization 'sealed' the faults, restricting the addition of large external fluid fluxes, thereby returning to closed system behavior, until the next large scale seismic event. The behavior of the faults probably switched back and forth between the two; a relatively closed system, mixing internally buffered fluids during minimal displacement, and an open system, allowing for large quantities of fluids (and

matter) to be introduced during larger seismic events, until mineralization would seal the fault and return to relatively closed system behavior.

Layered vein assemblages, textures, and REE patterns are consistent evidence of seismic pumping with open and closed system behavior. If only one geochemically homogenous fluid deposited the layered vein assemblages, the geochemistry of the layers would follow a set crystallization path, which would be reflected in the assemblages. The mineralogy would follow a predictable path as certain chemical species mineralized out of the fluids. Since this is not the case, fluids of slightly differing chemistries must have mixed with each other along strike, during small scale seismic pumping events, in a relatively closed system, resulting in alternating, sharply defined layers of varying, but similar mineral assemblages.

The REE concentrations from the bleached zones and Hogencamp layered vein assemblages are also evidence of relatively closed system behavior. REE patterns of the bleached zones and Hogencamp layered vein assemblages, parallel wall rock patterns, suggesting that no new large fluid fluxes were introduced during bleached zone alteration and layered vein mineralization, and it must have behaved as a relatively closed system. REE appear to have fractionated into the fluids, and eventually back into the bleached zones and layered assemblages, as concentrations progressively increase, but trends are consistently concordant to wall rock patterns. This is probably due to the incompatible REE fractionating into the fluids, and as alteration and mineralization occurred, less of the REE were incorporated into the crystallizing minerals, concentrating more REE in the fluids to be sequestered into the bleached zones and layers of mineralized vein. If large fluid fluxes were added to the system at this time, the REE patterns would likely deviate

from wall rock patterns, as any introduced fluids from an outside source would likely have different REE concentrations and would result in widely varying REE patterns.

We also hypothesize that the absence of a bleached zone at the Greenwood deposit is evidence of synchronous dilation and mineralization. We suggest that the dilational zone here didn't open during early bleached zone alteration conditions. The chemistry of the fluids was such, that by the time dilation occurred, the chemistry shifted from favoring exchange reactions, *i.e*. bleached zone alteration of wall rock, to layered vein mineralization. Exchange reactions probably only occurred during largest fluid fluxes, highest fluid and rock temperatures, and lowest fluid pH. Temperatures and fluid fluxes likely decreased, and pH increased by the time the zone dilated at the Greenwood deposit. If the dilational zone did open later than the others, the first fluids introduced were probably already neutralized through exchange reactions in other areas of the fault zone, restricting exchange reactions from occurring here, until layered vein assemblages subsequently mineralized. Furthermore, fluid fluxes probably weren't high enough for major element metasomatism, and no exchange reactions occurred between the fluids and wall rock.

Fluid Evolution

The fluids were likely derived from the metavolcanic country rock, through devolatization reactions associated with granulite facies metamorphism, coupled with other deeper crustal sources, shortly after the cessation of the Ottawan phase of the Grenvillian Orogeny (~1,024 Ma). According to Hemley (1959), the devolatization of various micas in the presence of chloride-rich fluids can form acidic solutions, as can other non-hydrous phases (e.g. Eugster, 1986; Holser and Schneer, 1961). Additionally, Holser and Schneer (1961) have shown that acidic solutions are very effective at

dissolving and transporting significant quantities of iron in solution. In fact, they have experimentally shown that even at low pressure and temperature, ~390°C and ~440 bars, a hydrochloric acid solution of ~0.0002 M (pH ~3.7) can contain upwards of 300 ppm of iron. They also recognized that an increase in acid concentration corresponds to an increase in the amount of iron the fluid can contain in solution. It can also be assumed that an increase in temperature and pressure would certainly lower the solubility even further, allowing larger quantities of dissolved iron to be transported in solution. In this way, acidic solutions could be derived from metavolcanic country rock, which would be free to liberate iron from ferromagnesian minerals into solution.

The high chlorine and fluorine content of the amphiboles and micas (Lupulescu and Gates, 2006; Lupulescu *et al.*, 2009), and the presence of sulfides in the vein minerals supports that the fluids were acidic. The high halogen content is also evidence of a complex, semi-aqueous source for the mineralizing fluids. The addition of diorite and pegmatite intrusions could have also contributed to the thermal and fluid input and aid in the dehydration processes. We consider that acidic solutions were derived from amphiboles and micas in the metavolcanic country rock which then liberated iron, and migrated towards the lower pressure fault zones.

$\delta^{18}O$ Oxygen isotopes from calcite from the Hogencamp and Bradley deposits yielded ranges between $\delta^{18}O$ 13.6 and 14.6 versus MSOW (M. Lupulescu, personal communication, October 25, 2006). This corresponds to the median of values for metamorphic derived fluids ($\delta^{18}O$ 5 - 25). These values are characteristic of crustal fluids and range into the granulite facices domain for carbonate minerals. Oxygen isotopes and observed mineral assemblages, both suggest that at the time of mineralization the fluids, not neccesarily the country rock, reached up to granulite facies conditions. As observed

in many of the deposits, clinopyroxene and orthopyroxene, and pyroxene and amphibole-rich assemblages are only stable in the granulite facies, limiting the conditions of formation of the deposits to ~700-800°C and ~5-10 kbars.

Bleached Zone

Once the dilational zones began opening, there was an influx of the acidic fluids. These fluids began chemical equilibration with the local wall rock through exchange reactions. In this way, the fluids internally buffered to the local chemistry and varied in composition depending on location. The fluids altered the wall rock to new assemblages and nucleated minerals on the vein walls. Small-scale seismically induced pumping events transported and mixed the fluids along strike, into different dilational zones. The fluids partially equilibrated to the new wall rock, contributing to the chemistry of the fluids and bleached zone alteration at the different dilational zones of the fault.

The primitive fluids involved in the chemical exchange reactions responsible for bleached zone alteration were modeled using wall rock bulk oxide geochemical and calculated mass transfer data (Fig. 17). By assuming a range of percentages where individual elements were either gained or lost into the fluids from the wall rock, allowed for the assumption of the composition of the earliest fluids before equilibration with local wall rock. Elements appeared to have a systematic behavior, either gaining or losing certain elements into the fluids based on the chemistry of local wall rock with few exceptions (*i.e.* calcium from the Bradley deposit, and the sporadic behavior of sodium). The primordial fluid composition was calculated as the chemical percentage ranges which were in partial equilibrium with the major oxides in local wall rock.

Silica ranges from about 55-65%, aluminum from 14-16%, calcium from 10-15%, iron from 10-12%, and magnesium from 4-7%. Lesser elements range from 2-5%

potassium, 1-5% sodium, 1-2% titanium, 1-1.5% manganese, and ~0.2% phosphorus. Assuming the lowest values of the percentage ranges, totaling ~98.2%, yields a composition of ~55% silica, ~14% aluminum, ~10% aluminum and calcium, ~4% magnesium, ~2% potassium, ~1% sodium, manganese, and titanium, and ~0.2% phosphorus, corresponding geochemically to a calc-alkline basaltic-andesite.

It should be emphasized that this is only the composition of a rock which would be in partial equilibrium with the primordial fluids. The percentages represent the relative abundances of the oxides in the fluids, not the actual composition of the fluid, which would otherwise be considered magmatic. This composition also validates a partial metavolcanic source of the fluids, as the assumed composition of the earliest fluids previous to equilibrium with local country rock, appears most similar to the composition of the metavolcanic country rock. The geochemistry of the primordial fluids also supports deposition of the volcanics in an island arc or marine magmatic arc setting, prior to granulite facies metamorphism.

In general, elements that appear in higher abundances in the wall rock show the greatest potential to be liberated into the fluids through exchange reactions, including silica, potassium, phosphorus, calcium, and sodium, to a lesser degree. Iron, magnesium, and manganese, on the other hand, almost all show mass gains in the bleached zones, regardless of the initial composition of the wall rock. Wall rock with the lowest concentrations in potassium, calcium, and phosphorus, generally show the largest gains in mass in these elements in the bleached zones.

The Hogencamp and Bradley deposits located in/or adjacent to calcium-rich country rock (calc-silicate/marble), exhibit large gains in calcium in the bleached zone relative to wall rock (6.5g/100g and 1.4g/100g respectively). This is reflected by the

calcium-rich assemblages formed in the bleached zone and early layered vein deposits. The Hogencamp bleached zone contains a calcite-rich, with scapolite and amphibole assemblage. The Bradley bleached zone, also had a large influx of silica (4.4g/100g), which is evident by the calc-silicate rich assemblage of scapolite, diopside, and calcite. The Hogencamp deposit, located within the silica-rich (61.4%) and potassium-rich (4.1%) metavolcanic unit, showed significant losses in the bleached zone of -3.8g/100g and -3.1g/100g, respectively. The Hogencamp and Bradley deposits also have similar fluid fluxes, ranging from 1.5 x 10^6 cm^3/cm^2 to 4.7 x 10^6 cm^3/cm^2 to alter wall rock to form the bleached zone, falling in the middle of the calculated flux ranges.

The Pine Swamp deposit located in the metavolcanic unit, adjacent to the quartzofeldspathic unit, is abundant in silica (~63.7%) and calcium (~6.3%) and low in potassium (~1.3%). The bleached zone gained iron (2.4g/100g), magnesium (1.2g/100g), potassium (1.0g/100g), and calcium (0.6g/100g), and lost silica (-1.4g/100g). This is manifested in the bleached zone by the alteration of pyroxenes to amphiboles, and the appearance of scapolite and minor biotite. The Pine Swamp bleached zone has the lowest range of calculated fluid fluxes between 5.3 x 10^5 cm^3/cm^2 to 1.2 x 10^6 cm^3/cm^2. The Surebridge deposit, located in the quartzofeldspathic unit, on average shows gains in all oxides. Though silica- (70.3%), and calcium- (4.0%) rich, significant additional quantities were added to the bleached zone (7.4g/100g and 1.8g/100g respectively), represented by an amphibole-dominated assemblage, also containing scapolite. Surebridge also has the highest calculated fluid fluxes, ranging from 2.9 x 10^6 cm^3/cm^2 to 6.7 x 10^6 cm^3/cm^2 to alter the bleached zone from country rock. The higher fluid fluxes calculated for the Surebridge deposit resulted in a higher degree of element mobility and mass transfer.

Regardless of wall rock composition all the bleached zones show significant gains in both iron and magnesium, ranging from 2.4g/100g to 5.3g/100g, and 1.0g/100g to 2.8g/100g respectively. This is manifested as ferromagnesian-rich mineral assemblages in the bleached zones, and the early layered vein deposits. Ferromagnesian-rich mineral assemblages are also observed well into the massive mineralized vein deposits. Additionally, all four of the deposits modeled show overall mass and volume gains into the bleached zone, ranging from ~3.1g/100g up to 18.1g/100g of wall rock, and 2.5% to 20.3% respectively (Figs. 18 & 19).

Rare earth element mobility during metasomatism has been highly debated, though it is clear that REE appear to be mobile in some circumstances, and immobile in others (Grauch, 1989). One large factor in REE mobility seems to be fluid acidity, as REE enrichment of hydrothermal solutions generally increases with decreasing pH (Michard, 1989). Acidic fluids proposed here would certainly aid in the mobilization of the REE into the fluids, and subsequently into suitable host minerals in the bleached zone and vein assemblages. In this case, all analyzed trace elements were mobilized during the hydrothermal process, and in most samples, REE trends appear similar to the host rocks patterns. Assuming relatively closed system conditions during bleached zone alteration, a metamorphic rocks REE content will directly mimic its protolith (Grauch, 1989), as acidic fluids leached REE from the wall rocks and deposited them in the bleached zone assemblages.

Analysis of samples Hogencamp-1 and Bradley-1 show the highest concentrations of rare earth elements, especially the LREE, also exhibiting the lowest values of HREE elements, possibly due to carbonate-rich inputs from adjacent country rocks. The large variance in wall rock compositions explains the differences in the rare earth element

concentrations between deposits, which generally reflect their mostly igneous protoliths. The negative Eu anomaly suggests that they fluids were depleted in Eu, as it was likely left behind in the source rocks and little to no plagioclase formed which could incorporate the highly incompatible element. The analysis of Bradley-3 shows that bleached zone REE concentrations differ significantly from wall rock. Although, reactive rocks such as carbonate-rich lithologies, like Bradley wall rock, may gain or lose significant amounts of REE during fluid/rock interactions (Lottermoser, 1992), and REE will only be preserved if suitable host minerals are formed in the bleached zone. Since suitable REE host minerals probably did not form in the bleached zone of this particular sample, REE are therefore depleted relative to wall rock.

A weak correlation is apparent between REE and major element mass transfer. Two of the analysis with larger overall losses in major elements, Surebridge-1 (-11.8%) and Hogencamp-1 (-5.4%), were enriched in REE in the bleached zone, mostly LREE and HREE. All other analyzed REE were depleted relative to wall rock, either with an overall gain or loss of major oxides. Bradley-3 had an overall volume gain of ~20.2%, which also had the greatest loss of REE. REE appear to behave opposite the major oxides, possibly due to the fractionation of the incompatible REE's into the fluids with the exception of Eu. However, no correlation is apparent between REE mobility and fluid flux. Fluid fluxes from the Hogencamp and Bradley deposits fall within the middle of the calculated values ranging between 1.5×10^6 cm^3/cm^2 – 4.7×10^6 cm^3/cm^2, however Bradley only lost REE and Hogencamp both gained and lost minor amounts of REE in the bleached zone. Fluxes from the Pine Swamp deposit had the lowest calculated ranges, as low as 5.3×10^5 cm^3/cm^2, and had only small losses in the REE. Calculated fluxes from the Surebridge deposit were at the higher end, up to 6.6×10^6 cm^3/cm^2, and

showed only minor gains of REE. In this case, it does not appear that REE mobility increased with fluid flux.

The bleached zone is absent in some localities (e.g. Greenwood), which leads us to speculate that the dilational zone here possibly opened later than the others. We consider that temperature of the country rock and fluid fluxes likely dropped, and the pH of the fluids rose before the Greenwood deposit dilated, limiting exchange reactions with the wall rock, therefore not allowing for bleached zone alteration to occur. Acidic fluids were likely neutralized through exchange reactions in other areas of the fault zone previous to dilation and introduction into the Greenwood dilational segment of the fault. Instead layered vein assemblages were deposited in direct contact with the wall rock. This may explain why the bleached zone is not observed here, in this case, the fault did not dilate under earliest bleached zone alteration conditions, and fluid fluxes were likely below the threshold of 10^6 - 10^8 cm^3/cm^2, the volume of flux necessary for major element metasomatism of wall rock at the Surebridge deposit.

Layered Vein

Chemical species in abundance in the local country rock contributed to the compositions of the earliest fluids that altered and precipitated minerals in the bleached zones, and mineralized layered and massive vein deposits. It is likely that these fluids migrated along the fault during small-scale seismic episodes, carrying chemically equilibrated fluids into different areas within the fault zones. Small displacements along the fault pumped fluids amongst the dilational zones in a relatively closed system, mixing and depositing layered vein assemblages. The faults behaved as a closed system over a distance along the fault zone, by means of a narrow or sealed fault plane, such that large fluid fluxes could not readily infiltrate and contribute to the chemistry of the system.

Larger seismic events and displacement would have dilated the structures further, inducing inward migration of fluids which would eventually deposit the massive vein assemblages.

Higher pressures permitted higher levels of ions to remain in solution in the narrow faults connecting the dilational zones (Eugster, 1986). Wall rock in these areas likely exhibited lithostatic pressure. As fluids migrated along the fault, they encountered different physio-chemical environments. Reducing fluid pressure from lithostatic, closer to hydrostatic pressure at the dilational segments of the fault, the solubility of mineral species decreased and they precipitated on the vein walls. Fluid pressures, though lower than the surrounding country rock, would have been high enough in the dilational structures that they could remain open at depth. The mixing of the fluids may have aided in the mineralization process, as changing the chemistry of the fluids, changed the solubility of certain species and also promoted precipitation. Layered vein deposition occurred after exchange reactions between wall rock and fluids ceased, as layered vein deposition occurred atop bleached zone assemblages, not directly on the wall rock.

The layered vein assemblages formed through a process similar to syntaxial vein growth (Durney and Ramsay, 1973), in that crystal growth was primarily on the vein walls inward. Crystal nucleation sites were mainly along the walls of the veins. However, also similar to composite vein growth (Durney and Ramsay, 1973), more than one mineral species was involved, most of which are found within the adjacent country rocks, and no preferred orientation of crystal growth is apparent at the wall contact. Also similar to composite growth, the minerals are arranged in layers, parallel to the vein walls. The processes at work were probably a combination of syntaxial and composite vein growth. Additionally, layered assemblages were likely formed in earlier volume

confined conditions, only allowing for fine-medium grained crystal growth and mineralization in layers during small-scale episodic dilation and pumping events.

The wall rock at the Hogencamp deposit (Fig. 22 A), for example, was first altered by the infiltration of hydrothermal fluids into the fault zone to create the bleached zone, during earliest dilation (Fig. 22 B). As the fault zones continued to dilate, fluids mixed and changed in composition and deposited amphibole/calcite-rich layered vein assemblages (Hv_1), adjacent to the bleached zone, during space confined conditions (Fig. 22 C). By the time the first layer of assemblages was deposited on the vein walls, bleached zone forming exchange reactions would have ceased, as the fluids were no longer in contact with original wall rock, and country rock temperature and fluid pH no longer permitted exchange reactions to occur. Small scale, episodic seismic events dilated the faults further and acted as a pumping mechanism moving and mixing fluids from one area of the fault zone into another, in a relatively closed system without any additional large scale fluid fluxes. Fluids varied in composition and flushed laterally and vertically, mixing the fluids and depositing the second layer (Hv_2) of layered amphibole and clinopyroxene-rich vein assemblages. With continued dilation and fluid mixing, further amphibole-rich layer Hv_3 and orthopyroxene/clinopyroxene-rich layer Hv_4 were deposited in the same manner (Fig. 22 C). Eventually the dilational zones opened much farther during larger seismic events, allowing for large scale fluxes to again enter the system, resulting in the massive deposits central to the veins (Fig. 22 D).

We consider that bulk oxide and REE geochemical data are consistent evidence of fluid mixing in a relatively closed system. Major element trends across the analyzed layers from the Hogencamp deposit (Fig. 11), do not show a continuous geochemical trend, instead they fluctuate, implying local mixing of fluids during seismic events.

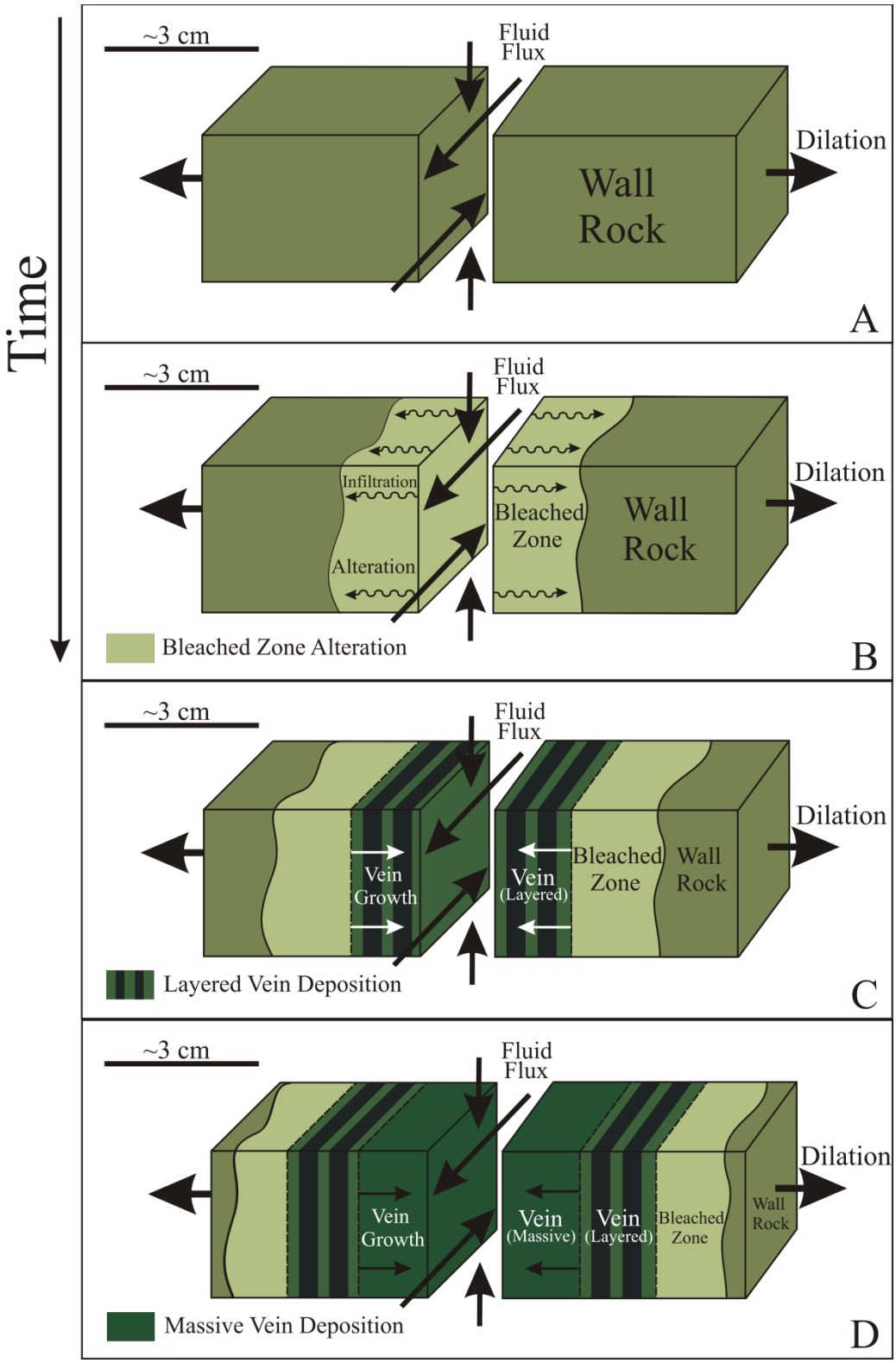

Figure 22. Schematic block model of the formation of the vein deposits. Fluids flushed into the dilational fault zone, altered wall rock, and deposited vein assemblages during episodic dilation (modified after Weisenberger and Bucher, 2010).

The more incompatible REE on the other hand, appear to fractionate into the fluids and are eventually incorporated into the layered deposits (Fig. 12). This leads to enrichment of the REE into the layered vein by removing the more compatible major elements through crystallization, which may reflect the general crystallization trends of the system. Fractionation of the incompatible REE into the fluids and deposition into the layered vein assemblages is also evidence that the system was relatively closed. REE trends parallel bleached zone values through all analyzed vein layers, if large outside fluid fluxes were introduced at this time, REE trends would likely deviate from wall rock and bleached zone concentrations. The fact that the major elements did not fractionate during crystallization, suggests fluids did shift and mix locally between dilational zones within the faults in a relatively closed system.

Introduction and equilibration of ferromagnesian-rich fluids into the faults resulted in the deposition of the early pyroxene/amphibole-rich assemblages. Local internally buffered fluids interacted in some localities, resulting in early clinopyroxene-rich layered and massive mineral assemblages in areas of calcium enrichment (e.g. Hogencamp and Bradley), amphibole-rich assemblages in areas of silica enrichment (e.g. Greenwood and Surebridge), and orthopyroxene-rich assemblages in localities increased mostly in iron and magnesium (e.g. Pine Swamp) (Table 4).

Though fluid fluxes were calculated for bleached zone alteration, fluxes could not be directly calculated for the mineralized deposit. Relatively smaller amounts of fluids were necessary to alter wall rock to bleached zone assemblages; it can be assumed that fluid ratios would have increased significantly to have deposited the layered vein assemblages. Fluids ratios would have increased to even greater volumes necessary to

liberate and transport the large amounts of iron to the fault zones, in order to deposit the massive vein assemblages, including the magnetite ore central to the vein deposits.

Massive Vein

Deformation continued during large scale seismic events, as the dilational structures opened much farther and the fault zones returned to open system behavior. Large cavities were created for significant volumes of the mineralizing fluids. The fluids became very iron and volatile rich by depleting other elements through crystallization, and deposited the massive magnetite ore with minor gangue and later interstitial minerals. Fluid pressure in these large dilational zones would have been lower than the lithostatic pressure of the surrounding rock. Iron ore-forming fluids encountered this pressure drop; the solubility of iron dropped and prompted magnetite precipitation. In addition, if the fluids were acidic, mixing of any carbonate-rich fluids, possibly derived from calc-silicate and marble country rock, would neutralize the fluids and also promote magnetite precipitation. In this way, pressure drops and neutralization reactions initiated crystallization in the massive zones by precipitating ions out of solution to form the massive magnetite deposits.

Extremely large volumes of fluid would be required to transport and deposit the enormous amounts of iron composing the magnetite ore. Fluid ratios were so extreme, that it depressed crystal nucleation sites, resulting in the coarse to massive magnetite and gangue minerals. High fluid ratios also aided in element mobility during mineralization, amplifying the ability to grow larger crystals. As mineralization occurred in the large fluid filled cavities, large, randomly oriented, euhedral crystals formed, e.g. clinopyroxene from the Hogencamp deposit.

The fluids were likely always very iron-rich, however during bleached zone and layered vein deposition, they also contained more of the other locally buffered chemical species, which allowed other ferromagnesian minerals to form, not just magnetite. Eventually these species were used up, leaving residual, extremely iron and volatile-rich fluids, which dominantly mineralized the massive magnetite. If further episodic fluid fluxes were added during massive vein mineralization, the result would likely be finer-grained deposits of varying chemistries which evolve with the fluids, not the observed massive assemblages, which had to form in a very volatile-rich environment.

Oxygen fugacity (fO_2) must have been sufficient enough as well, such that pure magnetite and the other gangue silicates were both able to mineralize in the core of the veins around the same time. Massive magnetite and gangue minerals (amphiboles/pyroxenes) crystallized first, during high oxygen fugacity conditions which eventually decreased as much of the iron oxidized to form magnetite. The massive gangue minerals also depleted other elements in the fluids further, leaving relatively more iron in solution to oxidize and form magnetite. The high concentration of iron oxide within the ore zone is evidence that the fluids were relativley oxidized at this time. Once the iron in the fluids oxidized to form the massive magnetite deposits, the fluids eventually switched from oxidizing to reducing conditions. Either a residual or an internally buffered late stage fluid overprinted the massive assemblages with the interstitial minerals quartz, calcite, and/or sulfides in a now reducing environment. In this way, the redox state of the fluids changed as mineralization evolved.

Locally equilibrated fluids mixed with ore forming fluids in a relatively open system and contributed to the massive gangue minerals with the magnetite ore. Clinopyroxene formed in areas of calcium enrichment (Hogencamp and Bradley),

amphibole-rich assemblages formed in deposits enriched in silica (Surebridge and Greenwood), and orthopyroxene- and sulfide-rich assemblages formed in deposits enriched dominantly in metal species (e.g. iron, magnesium, sulfur; Pine Swamp). In addition, fluids buffered to local chemistry of the host rocks also played a role in the late-stage cementing minerals. Interstitial calcite, quartz, and sulfide cement occurs in areas of calcium- (Hogencamp and Bradley), silica- (Greenwood and Surebridge), and sulfide-rich (Pine Swamp) country rock, respectively.

Temperatures must have been significantly high in order to liberate at transport iron to the fault zones. Argon dating of hornblende from massive Hogencamp vein yielded ages between ~914 - 922 Ma, thought to represent cooling ages (Gates *et al.*, 2006). The closure temperature of argon in hornblende is ~500-550°C (Dodson, 1973). This constrains the timing of massive vein mineralization towards the waning stages of strike slip movement in the Highlands (~924 Ma) (Gates and Krol, 1998), around a temperature of ~550°C. Biotite from the same location yielded and age of ~840 Ma (Gates *et al.*, 2006), and has an argon closure temperature of ~300°C (Harrison *et al.*, 1985). Therefore, 200-250°C of cooling took place between ~74 - 82 Ma, representing a slow rate of ~2.4 - 3.4° C/m.y. This rate would be consistent with temperatures in excess of ~700°C corresponding with the end of granulite facies metamorphism, the beginning of strike-slip deformation, and emplacement of diorite and the first generation of pegmatite intrusions (~1,024 - 1,008 Ma). This constrains the timing of synchronous deformation and mineralization of the vein type deposits between ~1,024 – 924 Ma. We suggest that temperature and pressure both progressively fell during deformation and mineralization in a period of uplift and unroofing, which aided the mineralization processes.

Model of Formation

During the later stages of dextral shearing and uplift (~1,008 - 924 Ma), temperature and pressure decreases and high fluid pressure caused the shear zones to cross the brittle-ductile transition and dilational right step-over structures formed within the zones. Country rock, still in excess of ~700°C from the waning stages of granulite facies metamorphism (~1,024 Ma), was intruded by diorites and associated pegmatites (~1,008 Ma), and later pegmatites. Hydrofluoric, hydrochloric, and sulfuric acidic fluids derived from amphiboles and micas in metavolcanic country rock liberated iron, migrated towards the fault zones, and filled the dilational fractures. Fluids ranged into granulite facies conditions, with temperatures in excess of 700°C, and pressures ranging from ~5 - 10 kbar, the conditions necessary to form the observed amphibole/pyroxene-rich assemblages.

These metamorphic fluids flushed into and filled the fractures and equilibrated with wall rocks through exchange reactions. Fluids were locally chemically buffered, enriched in elements that dominate the adjacent country rocks chemistry, e.g. calcium in areas of calc-silicate and marble, silica in areas of metavolcanic and quartzofeldspathic country rock. Varying degrees of seismically induced pumping of the fluids during episodic dilation moved and mixed the fluids along the fault zones. Mineralization along the faults eventually sealed fluids in the fault zones and dilational segments as the system eventually became relatively closed.

The earliest fluids altered wall rock into bleached zone assemblages during minimal displacement. Changes in chemistries into the bleached zone, at the wall of the vein, relative to unaltered country rock reflect the exchange of various chemical species to and from the buffered fluids. Partially buffered to the composition of local country

rocks, these fluids were transported and mixed along strike during small scale seismically induced pumping events, slightly dilating the structures further. Fluid fluxes were high enough to alter wall rock to distinguishably different assemblages in the bleached zone. The fluids encountered and mixed with fluids from other sections of the fault and changed in composition, finding favorable physical and/or chemical conditions for precipitation within the dilational areas in the fault zones.

Pressure drops and fluid mixing at the dilation segments of the faults caused certain species in the fluids to become supersaturated and prompted precipitation. A combination of syntaxial and composite vein growth precipitated minerals in the confined cracks, and resulted in the early layered vein deposits, primarily composed of alternating pyroxene- and amphibole-rich assemblages. Nucleation sites were primarily along the walls, and only allowed for fine to medium grained crystal growth. The layered vein assemblages provide mineralogical, textural, and geochemical evidence for seismic pumping and the mixing of fluids, and REE concentrations are evidence of relatively closed system behavior.

Local, internally buffered fluids also contributed to layered vein assemblages, as they mixed and flushed along the fault zones. In areas of calc-silicate country rock (Hogencamp and Bradley deposits), abundant calcium was mobilized into the fluids and resulted in calcium-rich vein assemblages. Calcium-enriched vein assemblages are dominated by clinopyroxene, calcite, amphibole, scapolite, and minor micas (Fig. 23). In quartzofeldspathic and metavolcanic country rock (Pine Swamp, Surebridge, and Greenwood deposits), silica was abundant, and most mobilized during mass transfer and vein deposition. Silica-enriched assemblages are dominated by amphibole, orthopyroxene, scapolite, quartz, and/or sulfides.

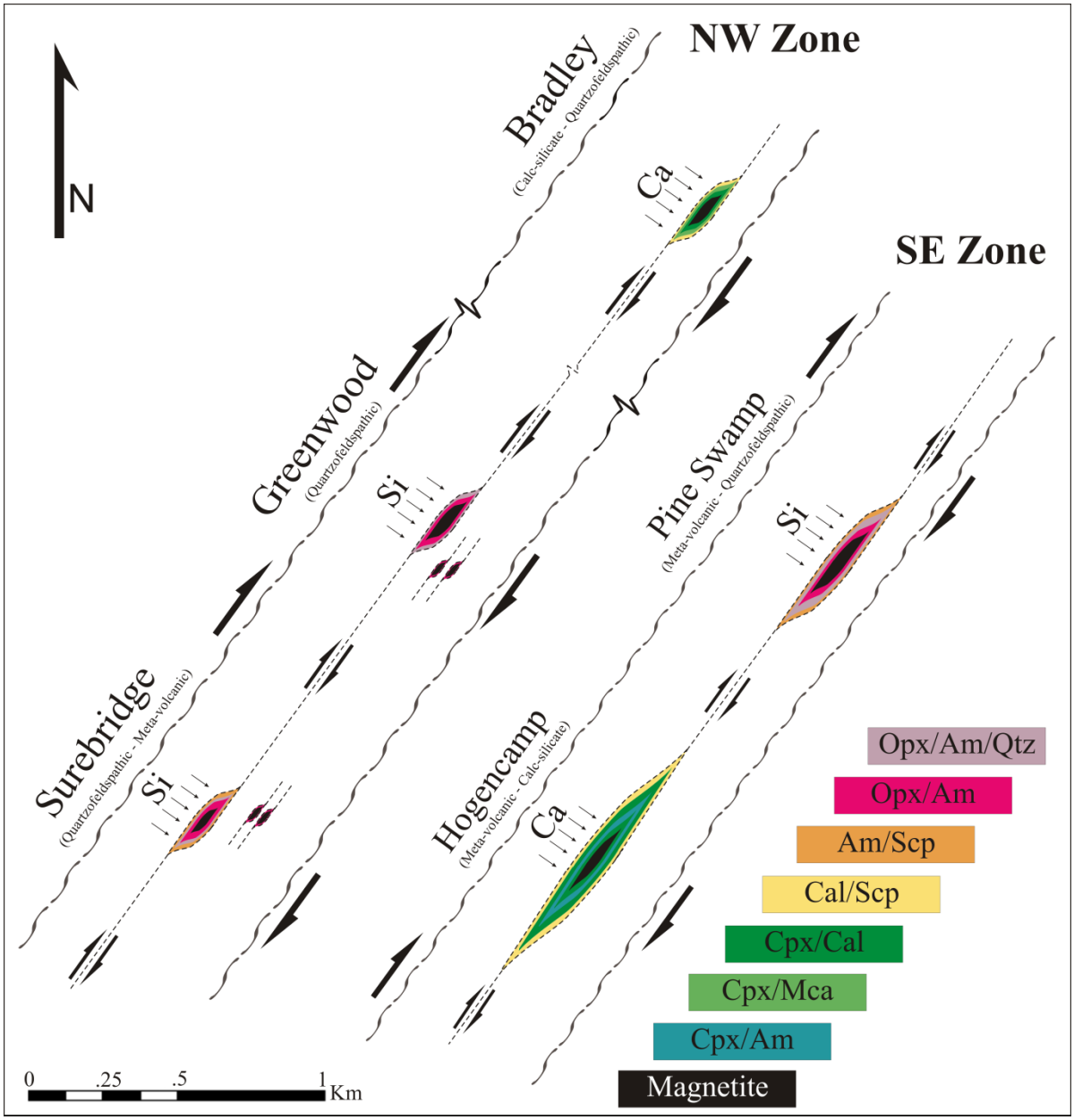

Figure 23. Schematic diagram of the vein deposit's dominate mineral assemblages, and sources of some chemical species.

With continued dilation and larger seismic events, large fluid volumes were introduced into larger fluid filled cavities, and the dominate mode of mineralization favored massive over layered deposits. Fluids became relatively very iron and volatile-rich as other chemical species were depleted through crystallization. Fluid ratios increased, depressing crystal nucleation sites and aiding in element mobility allowing

massive magnetite and ferromagnesian-rich assemblages, including euhedral crystals, to form in these cavities. Fluid pressure in these large cavities was also lower than surrounding country rock, dropping the solubility of iron, prompting mineralization. Mixing of any carbonate-rich fluids would have neutralized the acidic fluids, also lowering the solubility of magnetite, and promoting precipitation. Temperature and pressure decreases, and increases in oxygen fugacity limited the crystallization reactions, dominantly mineralizing magnetite and the few other gangue minerals.

As chemical species were depleted crystallizing the massive gangue minerals, the remaining dissolved iron oxidized and was deposited as the massive magnetite bodies. Locally buffered fluids also contributed to the gangue minerals of the massive assemblages. Clinopyroxene and interstitial calcite formed in deposits near calc-silicate and marble (Hogencamp and Bradley), and orthopyroxene/amphibole and interstitial quartz and/or pyrite formed in deposits near quartzofeldspathic and metavolcanic country rock (Pine Swamp, Greenwood, and Surebridge). Late in the massive vein mineralization process, conditions switched from oxidizing to reducing as iron was oxidized to form magnetite, and the late interstitial minerals overprinted the massive assemblages (calcite, quartz, and sulfides), in a reducing environment.

CONCLUSION

Geochemical and structural analysis of the mineralized faults leads to the interpretation of a model of formation for one type of massive magnetite ore bodies in the Hudson Highlands, NY (Fig. 24). During the late stages of deformation, dilational right step-over jogs formed in an open fracture system in the dextral shear zones. Acidic metamorphic fluids derived from metavolcanic country rock and deeper crustal sources were saturated in iron liberated from ferromagnesian minerals. The fluids flowed into

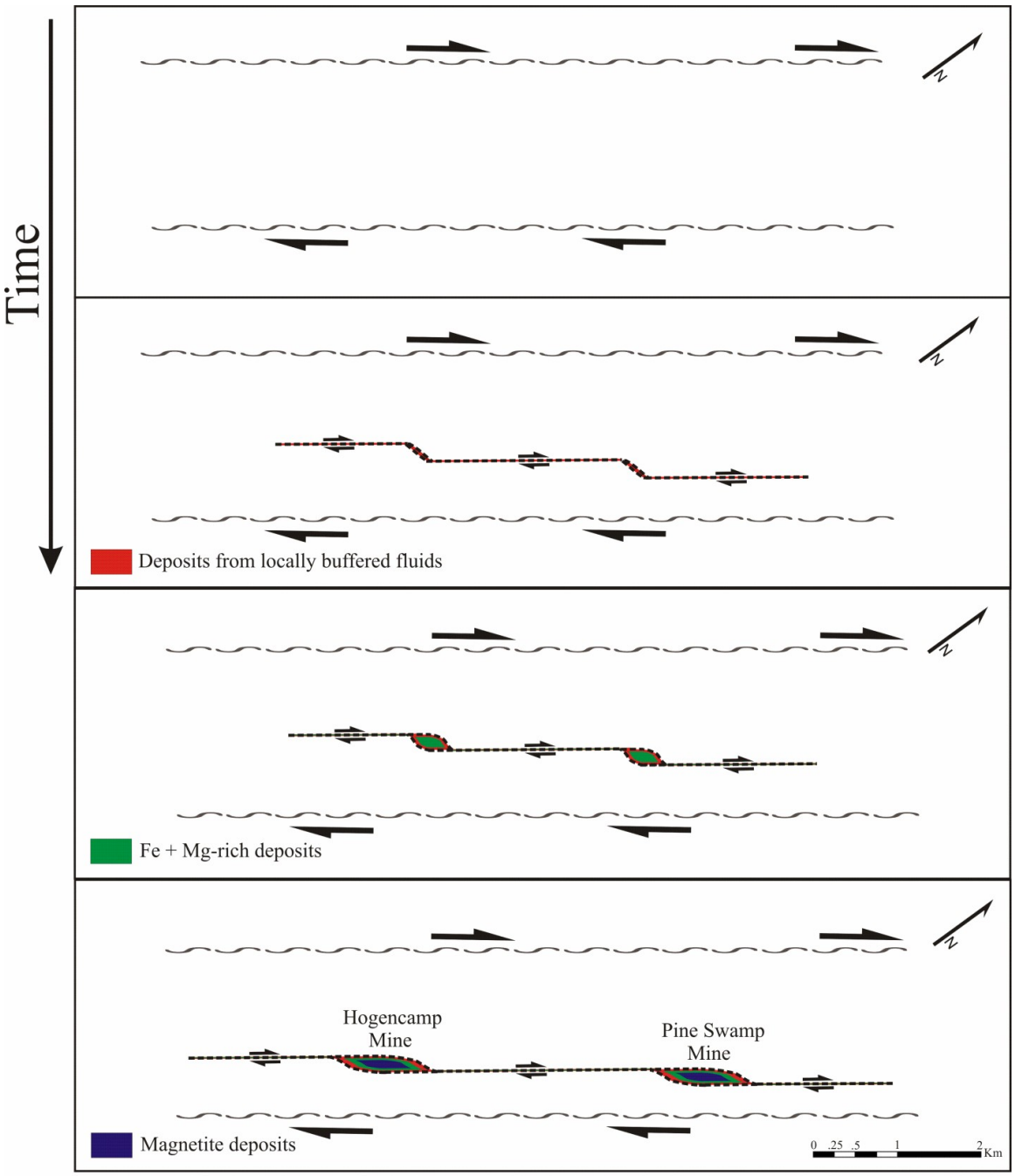

Figure 24. Model of the successive stages of the iron oxide vein deposits formation.

fractures, reacted with the wall rocks, and mobilized elements. Chemically buffered by the composition of the local country rock fluids migrated along strike during a series of seismically induced pumping events, during variable open and closed system behavior. As the structures episodically dilated, the fluids migrated into zones, encountered favorable physical and/or chemical conditions, and altered wall rock to bleached zone assemblages. During further dilation and seismic pumping events, fluids flushed and mixed along strike and deposited layered mineral assemblages in confined conditions in a relatively closed system. Deformation continued, and the dilational structures opened even farther as fluids became very iron-rich through the depletion of other elements. The massive mineral assemblages, including the massive magnetite in the core of the vein were than deposited. The assemblages reflect the changing chemistries of the fluids from changes in flux, fluid buffering source, chemical, and/or physical conditions. Latest pegmatites intruded the veins, possibly along some of the same pathways as the fluids.

Appendix-I

Table A-1. Southeastern shear zone bulk oxide geochemical results (w-wall rock, b-bleached zone, v-layered vein).

Oxide	Hogencamp-1								Hogencamp-2					Hogencamp-3						
(wt%)	Hw_1	Hw_2	Hw_3	Hb_1	Hv_1	Hv_2	Hv_3	Hv_4	Hw_1	Hw_2	Hw_3	Hw_4	Hb_1	Hw_1	Hw_2	Hb_1	Hv_1	Hv_2	Hv_3	Hv_4
SiO_2	64.56	70.14	70.20	55.96	48.00	47.13	45.98	44.76	59.62	57.63	57.03	55.64	53.06	58.37	58.68	50.88	47.22	43.97	42.52	40.44
TiO_2	0.62	0.34	0.33	0.31	0.22	0.32	0.32	0.32	1.07	1.34	1.07	0.93	2.02	0.57	0.58	0.38	0.40	0.38	0.37	0.42
Al_2O_3	13.73	12.21	13.00	14.05	11.18	7.93	7.49	8.62	16.36	14.82	15.87	17.13	14.89	14.25	11.95	10.41	7.99	9.31	5.32	4.97
Fe_2O3	4.84	3.66	5.01	9.69	13.06	13.95	12.10	11.59	7.21	8.48	8.40	9.75	10.86	6.60	7.39	11.96	10.90	11.60	18.77	23.68
MnO	0.20	0.13	0.16	0.23	0.25	0.27	0.20	0.17	0.06	0.06	0.05	0.04	0.05	0.13	0.18	0.24	0.27	0.19	0.21	0.21
MgO	2.00	1.55	1.63	3.80	6.08	8.59	11.73	13.25	3.84	4.26	5.10	5.81	6.06	3.62	4.92	7.22	11.79	13.92	13.47	12.43
CaO	3.46	3.37	4.75	11.93	17.58	20.45	21.42	18.58	7.14	8.77	8.28	7.41	9.40	9.73	10.16	15.91	20.49	17.19	18.62	17.81
Na_2O	2.42	2.63	4.27	4.23	1.86	0.91	0.65	0.91	5.35	4.81	5.03	5.11	4.41	2.57	2.33	0.86	0.68	0.80	0.30	0.33
K_2O	8.51	6.04	1.47	0.57	0.67	0.28	0.50	1.06	1.95	1.75	1.47	1.33	1.12	5.37	5.30	1.05	0.34	1.32	0.61	0.40
P_2O_5	0.13	0.08	0.11	0.24	0.49	0.79	1.30	1.02	0.36	0.23	0.19	0.12	0.18	0.17	0.06	0.20	0.14	0.01	0.01	0.01
Total	100.48	100.14	100.94	101.03	99.42	100.61	101.69	100.27	102.95	102.16	102.49	103.27	102.06	101.38	101.55	99.10	100.22	98.69	100.21	100.70

Table A-1. *cont.*

Oxide	Pine Swamp-1					Pine Swamp-2					Pine Swamp-3				
(wt%)	Pw_1	Pw_2	Pw_3	Pw_4	Pb_1	Pw_1	Pw_2	Pw_3	Pw_4	Pb_1	Pw_1	Pw_2	Pb_1	Pv_1	Pv_2
SiO_2	57.22	57.85	55.27	53.91	53.29	68.87	64.72	64.55	66.59	63.48	70.95	66.48	67.01	42.79	36.91
TiO_2	1.10	0.92	0.81	0.95	1.40	0.78	0.77	0.66	0.65	0.78	0.63	0.89	0.72	1.06	1.27
Al_2O_3	14.86	15.54	16.09	17.19	14.59	13.29	14.03	14.30	13.58	15.56	12.73	12.05	10.49	9.68	8.45
Fe_2O3	7.57	7.32	8.90	9.35	10.02	5.64	7.36	7.63	5.92	8.09	4.40	8.36	9.72	22.87	31.56
MnO	0.05	0.05	0.05	0.04	0.05	0.12	0.16	0.21	0.12	0.17	0.07	0.10	0.08	0.14	0.15
MgO	4.13	4.26	5.48	5.46	6.19	1.89	2.34	2.63	2.57	2.37	1.64	3.33	4.05	8.95	9.11
CaO	8.93	9.18	7.55	6.89	9.24	4.13	4.80	6.41	4.21	5.48	5.00	6.77	5.37	9.17	9.14
Na_2O	4.91	5.15	4.92	5.04	4.35	4.15	4.26	4.81	3.68	4.67	4.48	4.07	2.36	1.87	1.59
K_2O	1.66	1.32	1.12	1.27	1.17	1.03	1.48	1.11	2.83	2.47	0.88	0.80	2.95	1.84	1.36
P_2O_5	0.36	0.19	0.17	0.07	0.19	0.16	0.17	0.17	0.15	0.17	0.12	0.19	0.23	0.30	0.28
Total	100.78	101.77	100.36	100.17	100.50	100.06	100.11	102.49	100.31	103.24	100.90	103.03	102.97	98.67	99.82

Table A-2. Northwestern shear zone bulk oxide geochemical results (w-wall rock, b-bleached zone, v-layered vein).

Oxide	Bradley-1				Bradley-2						Bradley-3			
(wt%)	Bw_1	Bw_2	Bw_3	Bb_1	Bw_1	Bw_2	Bw_3	Bb_1	Bv_1	Bv_2	Bw_1	Bw_2	Bb_1	Bv_1
SiO_2	42.64	42.63	46.38	43.01	44.86	45.15	45.16	43.26	43.92	45.68	44.97	45.79	47.58	49.57
TiO_2	0.13	0.08	0.18	0.11	2.35	2.30	2.11	2.11	2.18	2.34	1.58	1.31	1.13	0.17
Al_2O_3	16.93	21.01	13.73	19.09	12.79	12.66	12.21	12.34	12.62	13.02	12.38	11.52	8.54	2.94
Fe_2O3	12.78	9.49	15.72	11.54	9.73	9.22	10.39	14.41	17.65	17.23	7.94	8.60	10.49	15.18
MnO	0.15	0.11	0.20	0.17	0.26	0.23	0.29	0.35	0.41	0.37	0.25	0.25	0.33	0.52
MgO	3.75	2.35	5.45	3.27	6.89	6.83	7.40	8.04	7.89	7.71	6.72	6.72	7.52	8.96
CaO	20.41	21.15	17.81	21.89	21.61	19.51	18.71	16.12	11.92	8.56	22.21	21.36	21.48	22.32
Na_2O	0.72	1.44	0.34	0.15	1.00	1.27	1.36	1.28	2.03	1.91	0.90	1.28	1.00	0.29
K_2O	0.09	0.15	0.29	0.07	0.60	0.80	0.81	1.25	2.33	4.34	0.18	0.25	0.33	0.15
P_2O_5	2.10	1.61	0.75	0.68	0.30	0.38	0.25	0.22	0.24	0.25	0.10	0.06	0.01	0.01
Total	99.71	100.01	100.86	99.98	100.40	98.35	98.71	99.37	101.20	101.40	97.23	97.14	98.42	100.10

Table A-2. *cont.*

Oxide	Surebridge-1					Surebridge-2				Greenwood-1				
(wt%)	Sw_1	Sw_2	Sw_3	Sw_4	Sb_1	Sw_1	Sw_2	Sw_3	Sb_1	Gw_1	Gw_2	Gw_3	Gv_1	Gv_2
SiO_2	66.65	69.58	70.68	70.94	59.39	74.12	68.32	73.02	43.38	50.86	49.34	46.31	42.36	37.29
TiO_2	0.45	0.34	0.34	0.31	1.00	0.30	0.66	0.36	0.58	0.87	0.80	0.80	0.57	0.44
Al_2O_3	13.50	13.58	14.03	14.24	13.97	12.32	16.52	13.50	10.34	16.22	15.39	15.21	9.95	7.18
Fe_2O3	10.23	6.68	5.39	4.98	11.28	3.61	3.45	7.31	24.91	11.59	13.46	17.17	24.45	35.38
MnO	0.12	0.09	0.07	0.08	0.16	0.04	0.03	0.03	0.22	0.13	0.15	0.16	0.23	0.23
MgO	2.36	2.00	1.67	2.26	4.20	1.42	0.52	0.68	7.80	6.49	6.22	6.32	7.69	7.05
CaO	4.36	4.17	4.03	5.01	7.13	3.55	3.83	3.52	9.68	10.88	11.23	10.17	11.87	10.57
Na_2O	4.16	4.33	4.50	4.45	3.89	4.06	5.69	4.56	2.37	3.62	3.50	3.20	1.71	1.19
K_2O	0.88	0.80	0.76	0.73	0.95	0.68	0.66	0.55	1.07	1.93	1.52	1.72	1.53	1.06
P_2O_5	0.08	0.05	0.05	0.08	0.29	0.04	0.09	0.09	0.06	0.31	0.27	0.29	0.18	0.05
Total	102.78	101.62	101.51	103.07	102.25	100.13	99.76	103.62	100.42	102.88	101.87	101.36	100.54	100.44

Table A-3. Trace element geochemical results (ppm) for select samples (w-wall rock, b-bleached zone, v-layered vein).

Sample	Hogencamp-1								Hogencamp-2					Pine Swamp-1					Pine Swamp-2				
(ppm)	Hw_1	Hw_2	Hw_3	Hb_1	Hv_1	Hv_2	Hv_3	Hv_4	Hw_1	Hw_2	Hw_3	Hw_4	Hb_1	Pw_1	Pw_2	Pw_3	Pw_4	Pb_1	Pw_1	Pw_2	Pw_3	Pw_4	Pb_1
Sc^{45}	10.94	7.80	7.40	9.17	6.02	7.78	8.13	9.83	26.52	32.57	29.20	30.11	40.12	30.06	30.77	31.13	30.81	37.48	13.71	16.33	18.37	16.32	13.07
V_{51}	54.18	34.91	29.35	36.97	28.83	33.39	31.14	30.22	155.47	204.09	162.34	182.35	267.33	180.61	156.58	172.06	187.31	227.00	74.26	83.19	85.47	85.98	72.77
Cr_{53}	38.93	27.19	25.66	28.70	21.17	20.02	21.09	28.82	45.21	55.25	186.66	281.59	107.60	64.30	51.97	261.96	332.33	133.23	59.79	56.81	60.38	53.58	46.15
Co^{59}	6.48	8.20	30.17	38.67	49.30	50.76	45.75	35.00	25.65	34.78	33.54	41.72	39.85	22.76	31.78	36.24	39.00	43.55	13.22	18.10	14.91	13.67	16.17
Ni^{60}	23.99	20.96	37.40	36.70	40.46	36.36	15.31	16.68	36.59	43.18	43.49	58.03	65.50	29.87	48.61	47.79	58.43	75.75	21.45	22.65	24.69	19.58	28.43
Ga^{71}	17.79	15.08	14.77	17.00	11.06	10.20	7.54	6.97	20.29	17.94	19.19	21.35	17.98	18.22	18.54	20.51	20.80	17.79	19.83	21.53	21.30	22.09	17.91
Rb^{85}	350.85	289.48	94.50	31.43	39.89	28.23	13.80	22.34	43.82	42.79	30.29	22.07	22.88	34.14	25.90	18.35	19.77	22.60	15.91	20.85	18.09	47.28	56.20
Sr^{86}	102.56	164.54	187.82	181.47	106.17	58.00	34.93	56.93	211.23	169.41	144.90	125.60	99.10	157.51	148.80	123.14	115.76	103.19	47.47	49.55	57.05	62.51	50.88
Sr^{88}	102.37	156.78	177.86	170.98	105.30	63.65	45.06	62.75	205.31	162.91	138.25	121.56	98.68	149.57	140.83	118.96	112.73	101.52	55.10	56.09	62.79	68.00	57.72
Y^{89}	38.07	29.66	54.05	49.64	44.22	61.20	80.90	83.88	41.13	43.95	42.48	39.42	31.28	44.23	39.62	48.20	43.23	33.20	57.67	62.75	36.44	38.29	41.68
Zr^{90}	109.18	97.15	113.92	101.32	89.60	116.86	143.03	143.62	40.80	27.96	28.76	28.64	41.73	32.14	43.06	27.73	26.21	35.03	49.16	31.25	28.53	47.08	75.74
Nb^{93}	10.81	6.28	19.15	11.59	-0.02	0.68	11.02	23.70	11.37	13.87	9.14	7.90	8.91	11.96	8.62	9.96	8.76	7.85	15.46	14.12	12.18	10.04	11.78
Cs^{133}	1.39	1.32	0.57	0.25	0.34	0.38	0.13	0.11	0.27	0.29	0.20	0.16	0.16	0.18	0.17	0.14	0.15	0.16	0.14	0.11	0.11	0.14	0.15
Ba^{135}	591.94	1148.49	1559.26	356.36	238.17	77.16	123.11	248.10	275.73	194.16	139.09	95.76	110.51	187.32	128.03	98.36	93.63	97.29	195.88	310.70	268.55	728.99	790.83
Ba^{137}	573.46	1109.97	1593.57	347.79	234.53	82.19	126.38	243.66	271.84	193.93	141.85	100.79	114.62	186.93	130.64	102.17	97.67	100.94	195.11	303.96	264.01	705.01	765.08
Ba^{138}	605.97	1163.18	1576.44	366.22	235.49	69.70	113.82	246.09	271.63	185.44	128.27	85.05	99.52	179.91	117.34	88.66	83.95	86.94	186.98	307.94	264.41	748.18	811.20
La^{139}	31.07	23.86	44.28	55.22	68.76	79.10	90.05	83.07	32.55	27.93	21.43	18.84	19.16	32.00	23.48	21.02	19.24	18.78	31.03	32.15	24.56	27.10	24.90
Ce^{140}	60.58	43.99	115.97	119.23	128.59	162.95	187.27	176.95	67.88	61.18	51.84	50.38	46.95	70.72	51.63	53.49	51.40	45.54	75.30	76.57	48.83	56.39	57.73
Pr^{141}	8.89	6.53	15.53	15.98	16.48	20.87	25.14	23.91	9.69	9.20	8.18	7.98	6.80	10.19	7.62	8.86	8.43	6.92	11.14	11.39	6.46	7.66	8.27
Nd^{146}	35.00	25.72	58.21	57.53	56.76	74.27	91.84	88.83	39.57	38.82	35.63	34.20	27.09	42.93	32.50	39.48	36.98	28.56	46.04	48.31	25.93	31.15	33.96
Sm^{147}	7.47	5.59	11.61	10.68	9.74	13.12	16.74	16.84	8.42	8.98	8.48	7.84	5.82	9.57	7.65	9.63	8.73	6.37	10.29	11.19	5.92	6.93	7.79
Eu^{151}	1.21	1.04	1.70	1.52	1.29	1.62	2.05	2.12	1.64	1.65	1.68	1.68	1.37	1.71	1.50	1.81	1.78	1.39	1.75	1.76	1.24	1.42	1.44
Eu^{153}	1.21	1.04	1.72	1.52	1.28	1.61	2.05	2.12	1.64	1.66	1.70	1.69	1.37	1.71	1.50	1.80	1.77	1.38	1.74	1.74	1.24	1.42	1.44
Gd^{158}	7.33	5.63	10.40	9.40	8.50	11.44	15.07	15.37	7.93	8.66	8.19	7.43	5.73	9.14	7.46	9.28	8.33	6.11	10.00	11.17	5.94	6.67	7.52
Tb^{159}	1.20	0.90	1.75	1.55	1.38	1.89	2.51	2.61	1.34	1.48	1.38	1.23	0.96	1.53	1.27	1.56	1.40	1.01	1.74	1.95	1.04	1.13	1.29
Gd^{160}	7.45	5.74	10.64	9.58	8.60	11.66	15.49	15.81	8.17	8.97	8.44	7.60	5.88	9.36	7.69	9.52	8.60	6.24	10.36	11.63	6.18	6.88	7.72
Dy^{163}	6.54	5.00	9.37	8.51	7.51	10.25	13.57	14.24	7.42	8.12	7.65	6.78	5.44	8.31	7.03	8.52	7.63	5.64	9.78	10.92	6.12	6.51	7.23
Ho^{165}	1.33	1.02	1.89	1.74	1.56	2.10	2.78	2.92	1.48	1.62	1.54	1.37	1.12	1.65	1.41	1.72	1.54	1.16	2.02	2.25	1.27	1.35	1.47
Er^{166}	3.39	2.62	4.89	4.64	4.20	5.57	7.29	7.67	3.86	4.18	4.04	3.65	2.98	4.21	3.67	4.50	4.07	3.09	5.40	5.86	3.46	3.60	3.88
Tm^{169}	0.48	0.37	0.70	0.70	0.64	0.84	1.07	1.13	0.57	0.61	0.60	0.56	0.46	0.61	0.55	0.67	0.61	0.47	0.80	0.87	0.53	0.54	0.58
Yb^{172}	2.96	2.35	4.49	4.77	4.49	5.71	7.06	7.34	3.65	3.93	3.89	3.69	3.07	3.95	3.58	4.40	4.04	3.17	5.24	5.53	3.58	3.56	3.72
Lu^{175}	0.45	0.37	0.66	0.77	0.73	0.89	1.04	1.06	0.53	0.58	0.57	0.55	0.48	0.58	0.54	0.65	0.61	0.49	0.77	0.80	0.55	0.53	0.54
Hf^{178}	3.34	3.12	3.58	3.48	2.98	3.30	3.75	4.09	1.06	1.13	1.17	1.16	1.53	1.26	1.40	1.25	1.19	1.39	1.72	1.28	1.05	1.54	2.40
Ta^{181}	0.61	0.28	1.27	1.25	0.05	0.18	0.58	1.20	0.93	0.74	0.81	0.50	0.62	0.60	0.59	0.86	0.62	0.57	0.76	0.71	0.77	0.66	0.57
Pb^{208}	19.95	16.27	8.48	8.16	6.82	3.94	3.17	3.57	1.46	1.20	0.85	0.46	0.73	1.15	0.93	0.55	0.61	0.51	4.14	4.66	4.92	6.31	5.67
Th^{232}	6.89	9.43	22.84	16.75	11.34	14.79	17.92	15.30	0.45	0.42	0.33	0.33	0.61	0.49	0.45	0.53	0.35	0.49	0.80	0.93	0.82	1.19	1.70
U^{238}	1.04	1.05	5.50	4.63	2.67	3.59	4.54	3.78	0.33	0.32	0.27	0.25	0.36	0.35	0.35	0.25	0.24	0.32	0.41	0.33	0.31	0.40	0.54

Table A-3. *cont.*

Sample	Surebridge-1					Bradley-1				Bradley-3			
(ppm)	Sw_1	Sw_2	Sw_3	Sw_4	Sb_1	Bw_1	Bw_2	Bw_3	Bb_1	Bw_1	Bw_2	Bw_3	Bb_1
Sc^{45}	15.90	14.82	13.15	16.97	25.78	19.55	10.15	22.68	8.10	32.73	26.57	16.89	11.08
V_{51}	56.09	32.05	36.60	33.61	161.15	19.14	12.22	24.92	17.18	218.00	159.91	117.84	96.06
Cr_{53}	20.34	16.59	13.82	19.28	64.00	9.06	6.78	8.74	6.50	76.82	77.87	48.53	21.51
Co^{59}	14.27	10.92	10.44	12.24	22.55	20.50	12.80	29.53	17.07	19.89	24.73	26.82	44.72
Ni^{60}	2.20	20.92	18.40	17.48	17.24	13.22	11.82	17.53	12.83	62.34	42.43	34.06	53.81
Ga^{71}	20.81	17.67	16.88	16.80	21.27	19.40	20.07	16.93	22.11	15.14	12.56	9.51	6.42
Rb^{85}	24.46	24.08	22.22	13.50	20.79	2.56	3.25	6.96	2.59	6.48	9.03	13.83	8.78
Sr^{86}	193.22	183.91	172.42	168.34	169.77	78.44	97.84	70.72	129.02	90.58	76.33	50.36	6.64
Sr^{88}	184.44	173.40	163.85	160.20	160.89	81.04	97.12	75.45	124.54	91.13	78.88	57.21	20.23
Y^{89}	30.88	32.86	34.16	43.54	81.86	52.67	34.13	33.49	31.43	47.80	37.36	31.81	8.46
Zr^{90}	21.07	17.81	13.19	18.31	31.92	26.24	14.82	41.86	31.21	96.48	83.86	81.46	39.38
Nb^{93}	2.32	2.40	2.60	4.65	9.53	1.29	0.38	1.09	0.63	12.18	11.73	12.88	0.06
Cs^{133}	0.11	0.13	0.13	0.11	0.09	0.46	0.51	0.33	0.17	0.54	0.53	0.92	0.30
Ba^{135}	343.28	324.29	284.50	237.57	241.61	-5.47	-1.72	34.11	2.96	48.14	44.29	58.07	48.02
Ba^{137}	334.85	316.43	278.79	233.72	238.26	3.91	7.18	41.93	12.05	54.72	50.57	63.93	54.51
Ba^{138}	352.10	331.52	284.72	231.16	239.18	-7.73	-4.44	28.04	-0.44	41.41	38.16	50.96	41.28
La^{139}	22.87	16.49	14.03	13.52	25.74	150.16	101.97	60.40	78.66	25.96	20.97	15.90	5.91
Ce^{140}	42.65	33.13	29.88	32.39	67.13	374.73	238.07	147.79	197.62	62.05	51.18	40.73	10.79
Pr^{141}	5.85	4.69	4.40	5.06	10.99	43.69	28.05	19.63	20.69	9.04	7.52	6.07	1.39
Nd^{146}	23.16	20.04	19.68	22.80	47.68	152.42	96.04	71.05	67.19	35.45	29.54	24.09	5.00
Sm^{147}	6.41	5.48	5.51	6.61	12.89	20.60	12.78	10.91	9.65	8.19	6.81	5.63	1.13
Eu^{151}	1.15	1.38	1.49	1.56	2.31	1.64	1.26	1.02	1.33	1.67	1.37	1.11	0.23
Eu^{153}	1.14	1.37	1.49	1.56	2.31	1.63	1.25	1.01	1.32	1.66	1.36	1.11	0.23
Gd^{158}	6.07	5.56	5.79	7.21	13.42	15.05	9.51	8.45	7.54	8.45	6.86	5.59	1.19
Tb^{159}	1.06	1.02	1.07	1.38	2.59	2.11	1.30	1.23	1.10	1.49	1.20	0.98	0.16
Gd^{160}	6.27	5.82	6.05	7.55	14.15	15.11	9.30	8.33	7.35	8.76	7.06	5.78	1.16
Dy^{163}	5.96	6.12	6.45	8.24	14.89	9.91	6.19	6.19	5.54	8.42	6.80	5.64	1.18
Ho^{165}	1.19	1.28	1.35	1.71	3.03	1.84	1.17	1.17	1.08	1.70	1.36	1.12	0.26
Er^{166}	3.09	3.39	3.57	4.57	8.17	4.30	2.81	2.83	2.69	4.26	3.42	2.87	0.76
Tm^{169}	0.46	0.51	0.53	0.69	1.29	0.54	0.36	0.38	0.36	0.58	0.47	0.40	0.14
Yb^{172}	3.00	3.27	3.37	4.60	8.80	3.02	2.03	2.17	2.08	3.38	2.74	2.38	1.04
Lu^{175}	0.44	0.48	0.49	0.66	1.25	0.38	0.27	0.28	0.27	0.42	0.35	0.32	0.21
Hf^{178}	0.66	0.61	0.50	0.71	1.46	1.02	0.50	1.31	0.81	3.01	2.80	2.79	1.25
Ta^{181}	0.08	0.09	0.08	0.51	1.10	0.42	0.34	0.39	0.29	0.72	0.70	1.29	-0.05
Pb^{208}	1.60	1.35	0.73	0.98	0.65	6.08	4.17	2.78	5.16	13.44	7.66	6.14	252.55
Th^{232}	0.17	0.10	0.04	0.04	0.10	130.61	69.68	29.15	31.91	11.52	9.97	8.38	0.44
U^{238}	0.20	0.19	0.18	0.18	0.19	9.67	5.50	2.69	2.51	5.08	4.21	3.61	0.19

Table A-4. Isocon results from both shear zones (change in volume %), across the wall rock-bleached zone boundary.

Oxide	Southeastern Shear Zone						Northwestern Shear Zone				
(Vol%)	Hogencamp			Pine Swamp			Bradley			Surebridge	
Sample	**1**	**2**	**3**	**1**	**2**	**3**	**1**	**2**	**3**	**1**	**2**
SiO_2	-24.3%	-0.6%	9.4%	3.7%	-11.5%	2.0%	-2.9%	-2.4%	34.1%	-15.3%	35.7%
TiO_2	-33.4%	97.8%	-15.9%	60.8%	0.0%	0.0%	-16.2%	-4.8%	0.0%	175.2%	0.0%
Al_2O_3	0.0%	0.0%	0.0%	0.0%	4.1%	-11.4%	9.8%	0.0%	-8.6%	0.0%	23.7%
Fe_2O3	98.5%	38.3%	115.4%	31.9%	12.5%	60.2%	-9.7%	49.7%	62.3%	63.9%	173.9%
MnO	32.8%	7.7%	96.7%	9.1%	4.6%	5.7%	12.3%	37.2%	69.4%	76.1%	37.1%
MgO	102.9%	37.4%	113.4%	39.8%	-7.3%	71.0%	-15.9%	16.1%	43.3%	101.0%	-8.1%
CaO	185.5%	28.2%	101.6%	24.0%	3.4%	-4.2%	9.6%	-17.7%	26.1%	60.9%	26.4%
Na_2O	25.7%	-6.5%	-55.6%	-5.3%	1.9%	-42.2%	-82.1%	7.8%	18.0%	-11.6%	23.7%
K_2O	-90.1%	-26.0%	-75.3%	-4.7%	41.6%	268.7%	-61.5%	69.9%	94.3%	19.1%	8.5%
P_2O_5	101.6%	-11.9%	123.5%	3.7%	-1.9%	55.0%	-54.8%	-24.4%	-83.8%	378.8%	105.7%
Total	-5.4%	10.82%	2.19%	7.16%	-8.96%	10.91%	-2.57%	43.36%	20.18%	-11.80%	34.42%

Table A-5. Densities used in mass balance calculations (g/cm^3). Wall rocks are averages.

SW Zone	Wall Rock	Bleached	**NE Zone**	Wall Rock	Bleached
Hogencamp-1	2.57	2.5	Bradley-1	2.97	3.02
Hogencamp-2	2.86	2.78	Bradley-2	3.08	2.79
Hogencamp-3	2.56	3.08	Bradley-3	3.33	3.59
Pine Swamp-1	2.74	2.79	Surebridge-1	2.76	3.1
Pine Swamp-2	2.87	2.91	Surebridge-2	2.47	2.52
Pine Swamp-3	2.56	2.44			

Appendix II

Major and Minor Elements

Subsequent sample preparation for major and minor element chemical analysis for all samples was carried out at the Department of Earth and Environmental Studies at Montclair State University, New Jersey. Pulverized samples were weighed out to 0.1000g (+/- 0.0005g), mixed with 0.4000g (+/- 0.0010g) of lithium metaborate ($LiBO_2$) flux, and placed in graphite crucibles. The sample crucibles were placed in a furnace at 1050°C for twenty minutes to form fused pellets and allow for chemical homogenization. After removing from the furnace, samples were immediately quenched in 50mL (+/- 0.5mL, weighed) 7% nitric acid (HNO_3) solution in Teflon beakers also containing Teflon magnetic stir bars. The sample beakers were then placed on magnetic stirring hot plates for about 20 minutes or until the fused sample was completely dissolved into solution. The resultant 500x diluted stock solution was then carefully filtered and added to 60mL Nalgene bottles, labeled and refrigerated. Master 4000x diluted solutions were then created from the 500x stock solutions to be analyzed on the instrument. In doing so, 6.5mL (+/- 0.3mL, weighed) of the 500x stock solution was added to 50mL (+/- 0.5mL, weighed) 2% nitric acid (HNO_3) solution in new 60mL Nalgene bottles, labeled and refrigerated. From the 4000x diluted master solutions, samples tubes were filled and placed in auto-sampling racks, the position of each sample entered into the instrument's computer data base, and the automated analysis initiated.

Samples were analyzed for bulk oxides and minor elements using a JY ULTIMA-C, multi-collector, ICP-OES at the ICP OES & MS Laboratory at Montclair State. For every rack of samples analyzed (n= 31 unknowns), 10 USGS standards were analyzed (USGS Analyzed Granite, G-2; Silver Plume Granodiorite, GSP-2; Glass Mt Rhyolite,

RGM-1; Guano Valley Andesite, AGV-2; Centerville Diabase, W-2; North Carolina Diabase, DNC-1; Quartz Lattice, QLO-1; Icelandic Basalt, BIR-1; Hawaiian Basalt, BHVO-2; and Columbia River Basalt, BCR-2), as well as three procedural blanks, prepared in the same manner. A single spiked drift monitor solution was also analyzed every fifth sample to account for instrumentation drift. Each individual sample solution was analyzed for bulk oxide major elements three times, than the results averaged to minimize analytical error. Any samples found to have an unacceptable margin of error (+/- 2% for bulk oxides) were re-prepared from powder and analyzed an additional three times, averaged, and once accepted, replaced the original results.

Trace Elements

Samples selected for trace element chemical analysis were prepared in a clean lab at the Department of Earth and Planetary Sciences at Rutgers University, Piscataway, New Jersey. Precisely weighed 0.2000g (+/-0.0005g) of pulverized sample was placed in 23ml Savillex beakers and saturated with concentrated nitric acid (HNO_3). 10 ml of 8N HNO_3, and 4 ml of concentrated 4N hydrofluoric acid (HF) were added, and placed in a ultrasonic bath for thirty minutes. Capped sample beakers were then placed on a hot plate overnight (~12-16 hours) at sub-boiling temperatures, to allow for the entire sample to dissolve. Samples were than uncapped and allowed to evaporate leaving a semi-dried yellow residue. 6 ml of 8N nitric acid was again added to the dried samples, placed in an ultrasonic bath for twenty minutes, and fluxed (sub-boiling) on a hot plate overnight. This process was repeated one additional time, evaporated, re-saturated in 8N HNO_3, and fluxed overnight. Samples were dried out one final time, 5 ml of 8N HNO_3 was added to re-dissolve the samples, and transferred to 15 ml Nalgene storage bottles. The Savillex beakers were rinsed with 5 ml DD H_2O and added to the 15 ml Nalgene storage bottles,

diluting the sample solution to 10 ml, yielding a 50x diluted stock solution. Samples solutions were vortexed and refrigerated.

Further trace element sample preparation and analysis was performed in a clean lab at the Department of Earth and Environmental Studies at Montclair State. 1 ml aliquots of the 50x stock solutions were added to 100 ml of DD H_2O, yielding a final ~4,500x diluted solution (precisely calculated). The sample solutions were then analyzed using a Thermo-electron X-7 series quadrupole mass spectrometer.

The suite of samples analyzed for trace elements consisted of 39 unknowns, including three independently prepared sample duplicates, as well as three USGS standards (USGS Analyzed Granite, G-2; Guano Valley Andesite, AGV-1; and Hawaiian Basalt, BHVO-2). Three other separately prepared USGS standards were also analyzed (Glass Mt Rhyolite, RGM-1; Centerville Diabase, W-2; and Icelandic Basalt, BIR-1). Additionally, five trace element spiked samples were analyzed, including solutions spiked in Ba, Ce, Nd, Pr, and Sm, and a single spiked drift monitor solution analyzed every fifth sample. Each sample was analyzed on three separate occasions, the results of which averaged and are reported in Table A-2.

REFERENCE

Anders, E. and Grevesse, N., 1989, Abundances of the elements: Meteoritic and solar: Geochim. Cosmochim. Acta., v. 53, p. 197-214.

Baker, D.R. and Buddington, A.F., 1970, Geology and magnetite deposits of the Franklin Quadrangle and part of the Hamburg Quadrangle, New Jersey: US Geological Survey Professional Paper 638.

Bayley, W.S., 1910, Iron mines and mining in New Jersey: Geological Survey of New Jersey Final Report Series VII.

Buddington, A.F., 1966, The Precambrian magnetite deposits of New York and New Jersey: Economic Geology, v. 16, p. 484-510.

Coelho, J., 2006, GEOISO - A Windows program to calculate and plot mass balances and volume changes occurring in a wide variety of geologic processes: Computers & Geosciences, v. 32, p. 1523-1528.

Collins, L.G., 1969, Regional recrystallization and the formation of magnetite concentrations, Dover Magnetite District, New Jersey: Economic Geology, v. 64, p. 17-33.

Dallmeyer, R.D., 1974, Metamorphic history of the northeastern Reading Prong, New York and Northern New Jersey: Journal of Structural Geology, v. 15, p. 325-359.

Dipple, G.M. and Ferry, J.M., 1992, Metasomatism and fluid flow in ductile fault zones: Contrib Mineral Petrol, v. 112, p. 149-164.

Drake, A.A. Jr., 1984, The Reading Prong of New Jersey and eastern Pennsylvania, An appraisal of rock relations and chemistry of a major Proterozoic terrane in the Appalachians, *In* Bartholomew, M.J. ed., The Grenville Event in the Appalachians and Related Topics, Geological Society of America Special Paper 194, pp. 94-109.

Dodd, R.T. Jr., 1965, Precambrian geology of the Popolopen Lake quadrangle, southeastern New York: New York State Museum and Science Service Map and Chart Series, No. 6, 39 p.

Dodson, M.H., 1973, Closure temperature in cooling geochronological and petrological systems: Contributions to Mineralogy and Petrology, v. 40, p. 259-274.

Durney, D.W., and Ramsay, J.G., 1973, Incremental strain measured by syntectonic crystal growths. *In* DeJong, K.A., and Scholten, R., eds., Gravity and tectonics. Wiley, New York, p. 67-96.

Eugster, H.P., 1986, Minerals in hot water: American Mineralogist, v. 71, p. 655-673.

Ferry, J.M. and Dipple, G.M., 1991, Fluid flow, mineral reactions and metasomatism: Geology, v. 19, p. 211-214.

Foose, M.P. and McLelland, J.M., 1995, Proterozoic low-Ti iron oxide deposits in New York and New Jersey, Relation to Fe-oxide-Cu-U-Au-rare earth element deposits and tectonic implications: Geology, v. 23, p. 665-668.

Gates, A.E., 1995, Middle Proterozoic dextral strike-slip event in the central Appalachians- Evidence from the Reservoir fault, NJ: Journal of Geodynamics, v. 19, p. 195-212.

Gates, A.E. and Krol, M.A., 1998, Kinematics and thermochronology of late Grenville escape tectonics from the central Appalachians: Geological Society of America, Abstracts with Programs, v. 30.

Gates, A.E., Valentino, D.W., Chiarenzelli, J., Gorring, M., and Hamilton, M., 2003, Field Trip to the Western Hudson Highlands: 2003 Long Island Geologists Conference, 30 p.

Gates, A.E., Valentino, D.W., Chiarenzelli, J.R., Solar, G.S., and Hamilton, M.A., 2004, Exhumed Himalayan-Type Syntaxis in the Grenville Orogen, Northeastern Laurentia: Journal of Geodynamics, v. 37, p. 337-359.

Gates, A.E., Valentino, D.W., Gorring, M., Thern, E.R, and Chiarenzelli, J., 2006, Rodinian collisional and escape tectonics in the Hudson Highlands, New York, *In* Pazzaglia, F.J., ed., Excursions in Geology and History: Field Trip**s** in the Middle Atlantic States: Geological Society of America Field Guide 8, p. 65-82.

Gorring, M.L., Estelle, T.C., and Volkert, R.A., 2004, Geochemistry of the Late Mesoproterozoic Mount Eve granite suite: Implications for Late to post-Ottawan tectonics in the New Jersey–Hudson Highlands, *In* Tollo, R.P., Corriveau, L., McLelland, J., and Bartholomew, M.J., eds., Proterozoic tectonic evolution of the Grenville orogen in North America: Geological Society of America Memoir 197, p. 505–523.

Grant, J.A., 1986, The isocon diagram—a simple solution to Gresens' equation for metasomatic alteration: Economic Geology, v. 81, p. 1976–1982.

Grant, J.A., 2005, Isocon analysis: A brief review of the method and applications: Physics and Chemistry of the Earth, v. 30, p. 997-1004.

Grauch, R.I., 1989, Rare earth elements in metamorphic rocks: Reviews in Mineralogy and Geochemistry, v. 21, p. 147-167.
Gresens, R.L., 1967, Composition–volume relationships of metasomatism: Chemical Geology, v. 2, p. 47–55.
Gundersen, L.C.S., 1986, Geology and geochemistry of the Precambrian rocks of the Reading Prong, New York and New Jersey - Implications for the genesis of iron-uranium-rare earth deposits, *In* Carter, L.M.H. ed., USGS Research on Energy Resources -1986 Programs and Abstracts, US Geological Survey Circular, v. 974, p. 19.
Gundersen, L.C.S., 2000, A backarc basin setting for a portion of the Proterozoic Reading Prong: Geological Society of America, Abstracts with Programs, v. 32, p. 21-22.
Gundersen, L.C.S., 2004, Tectonics and metallogenesis of Proterozoic rocks of the Reading Prong: Journal of Geodynamics, v. 37, p. 361-379.
Hagner, A.F. and Collins, L.G., 1955, Source and Origin of Magnetite at Scott Mine, Sterling Lake, New York: Science, v. 122, p. 1230-1231.
Hagner, A.F., Collins, L.G., and Clemency, C.V., 1963, Host rock as a source of magnetite ore, Scott Mine, Sterling Lake, New York: Economic Geology, v. 58, p. 730-768.
Harrison, T.M., Duncan, I.J., and McDougall, J., 1985, Diffusion of 40Ar in biotite: Temperature, pressure and compositional effects: Geochimica et Cosmochimica Acta, v. 49, p. 2461-2468.
Helenek, H.L., 1971, An investigation of the origin, structure and metamorphic evolution of major rock units in the Hudson Highlands: PhD Thesis, Brown University.
Hemley, J.J., 1959, Some mineralogical equalibria in the system K_2O-Al_2O_3-SiO_2-H_2O: American Journal of Science, v. 57, p. 241-270.
Holser, W.T. and Schneer, C.J., 1961, Hydrothermal Magnetite: Geological Society of America Bulletin, v. 72, p. 369-386.
Hotz, P.E., 1954, Some magnetite deposits in New Jersey: US Geological Survey Bulletin, 995-F, p. 201-254.
Lister, G.S. and Snoke, A.W., 1984, S-C mylonites: Journal of Structural Geology, v. 6, p. 617-638.
Lottermoser, B.G., 1992, Rare earth elements and hydrothermal ore formation processes: Ore Geology Reviews, v. 7, p. 25-41.
Lupulescu, M. and Gates, A.E., 2006, Iron deposits from Hudson Highlands, NY: Systematics, mineralogy, mineral chemistry and tectonic setting: Geological Association of New Jersey Field Guide and Proceedings, v. 23, p. 46-59.
Lupulescu, M.V., Rakovan, J., Dyar, M.D., Robinson, G.W., and Hughes, J.M., 2009, Fluoro-potassichastingsite from the Greenwood Mine, Orange County, New York: A new end-member calcic amphibole: The Canadian Mineralogist, V. 47, p. 909-916.
McCaig, A.M., 1987, Deformation and fluid-rock interaction in metasomatic dilatant shear bands: Tectonophysics, v. 135, p. 121-132.
Michard, A., 1989, Rare earth element systematic in hydrothermal fluids: Geochimica et Cosmochimica Acta, v. 53, p. 745-750.
Oliver, N.H.S., 2001, Linking of regional and local hydrothermal systems in the mid-crust by shearing and faulting: Tectonophysics, v. 335, p. 147-161.
Puffer, J.H., 2001, Five types of Proterozoic magnetite deposits in the New Jersey Highlands: Society of Economic Geology Guidebook Series, v. 35, p. 103-110.
Puffer, J.H. and Gorring, M.L., 2005, The Edison magnetite deposits in the context of pre-, syn-, and post-orogenic metallogenesis in the Grenville Highlands of New Jersey: Canadian Journal of Earth Sciences, v. 42, p. 1735-1748.
Schleicher, A. M., Tourscher, S.N., van der Pluijm, B.A., and Warr, L.N., 2009, Constraints on mineralization, fluid-rock interaction, and mass transfer during faulting at 2–3 km depth from the SAFOD drill hole: Journal of Geophysical Research, v. 114, B04202.
Sibson, R.H., Moore, J.M., and Rankin, A.H., 1975, Seismic pumping-a hydrothermal transport mechanism: J Geol. Soc. London, v. 131, p. 653-659.
Sibson, R.H., 1985, A note on fault reactivation: Journal of Structural Geology, v. 7, p. 751-754.
Sims, P.K., 1958, Geology of the Dover magnetite district, Morris County, New Jersey: US Geological Survey Bulletin, 982-G, p. 245-305.
Volkert, R.A. and Drake, A.A. Jr., 1999, Geochemistry and stratigraphic relations of Middle Proterozoic rocks of the New Jersey Highlands: U.S. Geological Survey Professional Paper 1565-C, 77 p.

Volkert, R.A., 2001, Geologic setting of Proterozoic Iron, Zinc, and Graphite Deposits, New Jersey Highlands: Society of Economic Geology Guidebook Series, v. 35, p. 59-73.

Volkert, R.A., Aleinikoff, J.N., and Fanning, C.M., 2010, Tectonic, magmatic, and metamorphic history of the New Jersey Highlands: New insights from SHRIMP U-Pb geochronology: Geological Society of America Memoirs, v. 206, p. 307-346.

Weisenberger, T. and Bucher, K., 2010, Mass transfer and porosity evolution during low temperature water–rock interaction in gneisses of the simano nappe: Arvigo, Val Calanca, Swiss Alps: Contrib Mineral Petrol, DOI: 10.1007/s00410-010-0583-2.

Winter, J.D., 2001, An Introduction to Igneous and Metamorphic Petrology. Prentice Hall, Upper Saddle River, New Jersey, first edition, 697 pp.

VITA

Michael J. Kalczynski

1981	Born May 20th, Buffalo, New York.
2002-2005	Attended Eire Community College, Williamsville, New York.
2005	A.S. in Applied Science, Eire Community College.
2005-2007	Attended Buffalo State College, Buffalo, New York.
2007	Geologic field assistant, Buffalo State College, Buffalo, New York.
2007	Teaching assistant, Buffalo State College, Buffalo, New York.
2007	B.S. in Geology, Buffalo State College.
2007-2012	M.S. Student, Rutgers University, Newark, New Jersey.
2007-2012	OEDG Program coordinator, Rutgers University, Newark, New Jersey.

Publications

Kalczynski, M.J., and Gates, A.E., 2012. Hydrothermal mass transfer and magnetite mineralization in dilational shear zones, western Hudson Highlands, NY. *Geological Society of America, Abstracts with Programs* **44**.

Gates, A.E., and Kalczynski, M.J., 2012. Using ground penetrating radar to attract minority students to geosciences in Newark, NJ. *Geological Society of America, Abstracts with Programs* **44**.

Kalczynski, M.J., Gates, A.E., Gorring, M.L., and Lupulescu, M.V., 2009. Hydrothermal alteration, mass transfer and magnetite mineralization in dextral shear zones, western Hudson Highlands, NY. *New York State Geological Association Field Trip Guidebook* **81**.

Kalczynski, M.J., and Gates, A.E., 2009. Hydrothermal alteration, mass transfer and magnetite mineralization in dextral shear zones, western Hudson Highlands, NY. *Geological Society of America, Abstracts with Programs* **41**.

Gates, A.E., and Kalczynski, M.J., 2009. Making geosciences "real" for urban youth in Newark, NJ. *Geological Society of America, Abstracts with Programs* **41**.

Kalczynski, M.J., and Solar, G.S., 2008. Structural and mineralogical variations associated with the south-western contact of the Sebago Pluton with the Sebago Migmatite Domain, SW Maine: Results from new mapping. *Geological Society of America, Abstracts with Programs* **40**.

Kalczynski, M.J., and Solar, G.S., 2007. Fabric analysis using point counting: A new use for an old tool? *Geological Society of America, Abstracts with Programs* **39**.